ELSEVIER

Contents lists available at ScienceDirect

Renewable and Sustainable Energy Reviews

journal homepage: www.elsevier.com/locate/rser



Uncertainty models for the structural design of floating offshore wind turbines: A review

Mahyar Ramezani ^a, Do-Eun Choe ^{a,*}, Khashayar Heydarpour ^a, Bonjun Koo ^b

- ^a Department of Civil Engineering, New Mexico State University, 3035 South Espina St., Las Cruces, NM, 88003, USA
- ^b Floater Advanced Simulation and Technology, Technip Energies, Houston, TX, 77079, USA

ARTICLE INFO

Keywords:
Renewable energy
Floating offshore wind turbine
Uncertainty model
Probabilistic modeling
Life-cycle reliability
Corrosion and fatigue deteriorations

ABSTRACT

Floating offshore wind turbines have arisen as a promising option to access massive wind energy resources in deep water, where the existing fixed-type offshore wind turbine is no longer practical. However, due to the nature of the oceanic environmental conditions, large uncertainties are involved in the aerodynamic/hydrodynamic calculations, which are coupled with those within the structures and materials. This not only threatens its reliability but also drastically increases the manufacturing cost of floating offshore wind turbines. To understand the uncertainty within the system and properly predict its reliability, first, the uncertainties involved in the environments and subsystems need to be defined. Therefore, this paper aims to provide an extensive review of the uncertainty models involved in the structural design of floating offshore wind turbines. The presented uncertainties within the structures include those inherent in the material and geometrical/mechanical properties of the wind turbine, floating structures, and mooring lines. The uncertainties within hydrodynamics include empirical parameters and nonlinearities involved with the hydrodynamics modeling of the floaters. Within the environmental loads, the parameter uncertainties as well as the randomness of wind and wave loads are presented. The uncertainties growing over time caused by fatigue, corrosion, and climate hazards are also discussed. In addition, the correlation between the random variables, such as the correlation of the wind and wave, is presented. Finally, the method of treating those uncertainties is discussed, including the probabilistic model which incorporates the uncertainties and the correlations between the random variables, as well as modeling errors.

1. Introduction

There is a pressing need to shift toward renewable energy resources to mitigate the catastrophic climate change effects resulting from the increased greenhouse gas (GHG) emissions due to the burning of fossil fuels. Among all, wind energy is the fastest-growing renewable source. The global cumulative wind energy capacity reached 837 GW in the year 2022, exhibiting a year-on-year growth of 12% [1], yet wind energy contributes to less than 4% of the total energy produced in the United States [2]. According to the U.S. Department of Energy, wind energy (both onshore and offshore) would contribute to about 35% of the U.S. electricity demand (i.e., 404 GW) by 2050, avoiding 12.3 gigatonnes of GHG emissions [3]. For a wind turbine to be utilized as an efficient renewable energy source, it is necessary to secure continuous and efficient energy production. From this point of view, it is essential to locate a site that can maintain a constant or higher wind speed for wind power

generation. Because winds are stronger and steadier at seas than they are on land, it is anticipated that offshore wind power installation occupies increasing clean energy industry capacity [4]. In addition, offshore power generation does not suffer from disadvantages such as space availability, noise, and aesthetics. The generation capacity of offshore wind turbines (OWTs) in Europe was nearly 22.1 GW by the end of 2019, with a projection of 70 GW by the year 2030 [5]. Currently, the offshore wind energy market is dominated by stationary (or fixed-type) foundations including monopiles, jackets, tripods, and gravity-based [6]. The stationary OWTs, however, require sites with relatively shallow water depth (usually smaller than 50 m), where sites with abundant wind conditions are inevitably limited [7]. In contrast, floating offshore wind turbines (FOWTs) with mooring lines and anchors including Tension Leg Platform (TLP), spar-buoy, semi-submersible, and barge-type could be deployed in deep water (up to 1000 m), generating substantial untapped wind energy [7,8]. The world's first FOWTs (five spar-buoys turbines) were installed in Scotland in 2017 [9]. According to the National

E-mail address: dchoe@nmsu.edu (D.-E. Choe).

^{*} Corresponding author.

Abbrevi	ations and nomenclature:	WRF	Weather Research and Forecasting
		NWS	National Weather Service
GHG	Greenhouse Gas	NOAA	National Oceanic and Atmospheric Administration
OWT	Offshore Wind Turbine	NCEP	National Centers for Environmental Prediction
FOWT	Floating Offshore Wind Turbine	CFSRR	Climate Forecast System Reanalysis Reforecast
TLP	Tension Leg Platform	FAST	Fatigue, Aerodynamics, Structures, and Turbulent
IEC	International Electrotechnical Commission		Simulation Tool
DNV	Det Norske Veritas	IAV	Inter-annual Variability
ABS	American Bureau of Shipping	FD	Drag Force
LRFD	Load and Resistance Factor Design	FI	Inertia Force
PSF	Partial Safety Factor	K-C	Keulegan-Carpenter Number
PDF	Probability Distribution Function	H_s	Significant Wave Height
COV	Coefficient of Variation	MSL	Mean Sea Level
σ	Standard Deviation	T_p	Wave Peak Period
GM	Graphical Method	T_{02}	Conditional Mean Period
MLM	Maximum Likelihood Method	E	Elastic Modulus
LSM	Least Square Method	ρ	Density
EPFM	Energy Pattern Factor Method	G	Shear Modulus
MM	Moment Method	ν	Poisson's Ratio
MMLM	Modified Maximum Likelihood Method	$\varphi^{'}$	Soil Friction Angle Property Variability
EM	Empirical Method	$f(H_s)$	Marginal Distribution of Significant Wave Height
EEM	Equivalent Energy Method	$f(T_{02} H_s)$	Distribution of the Mean Zero-crossing Period Conditional
EML	Empirical Method of Lysen	3 (==1 =/	on Significant Wave Height
EMJ	Empirical Method of Justus	$f(H_s, T_{02})$	Joint PDF of Significant Wave Height and Mean Wave
LTF	Linear Wave Force Transfer Function	,,	Period
QTF	Quadratic Sum and Difference Wave Force Transfer	ν_z	Mean wind speed at various heights
	Function	$ u_{z_0}$	Mean wind speed at the height of $z_0 = 10 \text{ m}$
κ	Shape Parameter	α	Wind shear exponent
с	Scale Parameter	$v_{z,SS}$	Sub-surface current speeds at a position of z below sea level
Y	Location Parameter	$v_{z,NS}$	Near-surface current speed at a position of z below sea
μ	Mean value	,	level
Y	Shape Parameter for Gamma Distribution	FORM	First-Order Reliability Method
θ	Rate Parameter for Gamma Distribution	IFORM	Inverse First-Order Reliability Method
K	Concentration Parameter for Von Mises Distribution	SORM	Second Order Reliability Method
$I_0(K)$	Modified Bessel function	RSM	Response Surface Method
E[C(t)]	Mean Capacity	MCS	Monte Carlo Simulation
D	Demand	MVFOSM	Mean Value First Order Second Moment
σ_o	Initial Standard Deviation	EGRA	Efficient Global Reliability Analysis
$\sigma(t)$	Standard Deviation at Time t	AK-MCS	Active Learning Reliability Method Combining Kriging and
X	Random Vector		Monte Carlo Simulation
g(X)	Limit State Function	ULS	Ultimate Limit State
MPP	Most Probable Point	FLS	Fatigue Limit State
β	Reliability Index	SLS	Serviceability Limit State
FEA	Finite Element Analysis	ALS	Accidental Limit State
SHM	Structural Health Monitoring		
CM	Condition Monitoring		

Renewable Energy Laboratory, the total potential production capacity of OWTs is double the United States' annual power consumption (4000 TWh per year), where 42% of the potential power might be generated from fixed-type turbines and the remaining 58% could come from FOWTs. Tapping into this lucrative market of \$70 billion by 2030, FOWTs are under extensive research and development worldwide. It is worth noting that due to technology and cost constraints, FOWTs are still in their infancy [4]. It is estimated that FOWTs could only generate between 4.0 GW and 5.0 GW of energy in Europe by 2030 [10]. For rapid development, a good understanding of inherent engineering challenges associated with FOWTs is therefore needed.

As FOWTs are incrementally deployed to deep waters with an increased rotor diameter and tower height, they could inevitably experience more significant dynamic motions and responses throughout the course of their service life [11]. The highly nonlinear dynamic motions and the response of FOWTs due to the coupled effects of aerodynamics,

hydrodynamics, mooring dynamics, etc. make their design much more complex than onshore and fixed-type OWTs. In the meantime, severe environmental conditions (e.g., wave, current, and wind loads) and their significant uncertainties in the deeper ocean aggravate the design complexity of FOWTs. Also, the effects of fatigue reliability on the FOWT structures should not be overlooked [12]. In the period of 2000-2020, human errors (e.g., design deficiency and fabrication/construction defects) and inadequate safety margins to accommodate uncertainties were the main reasons for wind turbine failures [13]. Traditionally, the available international design standards and codes consider load factors, such as partial safety factors (PSFs) and Load and Resistance Factor Design (LRFD), to account for uncertainties in a deterministic manner under various loading conditions. However, this design simplification using existing LRFD or PSFs may lead to over-design with undesired expenses in most cases [14]. Besides, the applicability of PSFs for FOWT structures might be questionable because the uncertainties arise from

the continuous cyclic hydrodynamic and aerodynamic loads, resulting in nonlinear behaviors [15]. An alternative approach is to design FOWT structures considering both aleatory and epistemic uncertainties in variables in a stochastic manner with proper types of distribution functions. Non-deterministic (probabilistic) structural reliability analysis might be used to properly estimate the target reliability index to be integrated into the conventional design codes, achieving certain safety levels in terms of fatigue and ultimate failure criteria, in addition to inspection/maintenance planning. Yet, the reliability analysis is merely referred to in this context [16,17]. Compared with the deterministic approach, this method may take into account the random nature of the sea state, allowing the identification of the worst conditions which are essential for the reliable design of FOWTs. However, very limited studies are available that extensively account for FOWT environmental, material, and geometric stochastic uncertainties [18,19]. Therefore, the objective of this work is to summarize and quantify various uncertainties involved in the design of FOWTs such as nonlinear environmental loadings, turbine blades, turbine material, soil properties, fatigue, etc., which significantly affect the FOWT reliability. The findings may be used to calibrate the existing load factors or certain loading conditions, avoiding their generalization which is a key step to increasing the reliability of FOWTs.

2. Uncertainties & uncertainty models

Reliable power generation can significantly reduce the cost of energy for FOWTs. Nevertheless, there are still many sources of uncertainties in the FOWT industry because of the lack of knowledge, the nature of the nonlinear dynamic system, lacking measurement capability, etc. Toft and Sørensen [20] categorized sources of uncertainties related to wind turbine into four groups: 1) physical, 2) model, 3) statistical, and 4) measurement uncertainties. Uncertainties in probabilistic modeling can be categorized into two types: epistemic uncertainty (reducible) and aleatory uncertainty (irreducible). Epistemic uncertainties arise from a lack of knowledge, our decision to simplify matters, measurement errors, and a small number of observations [21]. Aleatory uncertainties are inherent within the nature of the system, which therefore cannot be reduced. These uncertainties can often be modeled in the form of random variables that express environmental loads (aerodynamic and hydrodynamic loads), geometrical and mechanical properties within the structures, soil properties, and growing uncertainties over time. To improve the reliability, knowledge of the types of probability distribution and characteristic values of the random variables (i.e., how these uncertainties propagate through the models) is vital. Non-probabilistic uncertainty models, such as fuzzy logic, interval analysis, possibility theory, and belief functions, provide an alternative approach to quantifying uncertainty, especially in cases where limited or incomplete information is available [22]. These models enable the representation and reasoning of uncertainty without relying on explicit probability distributions, making them useful tools in addressing epistemic uncertainty in complex systems or when dealing with sparse data. It should be noted that epistemic uncertainties can be reduced throughout the design process, data collection, and measurements.

This section provides a comprehensive review of various uncertainty models and/or variability quantified in existing literatures. In Section 2.1, we discuss the parameter uncertainties within the environmental loads, which will determine the uncertainties of structural *demands* of FOWTs. Section 2.2 presents those uncertainties inherent in the structural *capacity* of FOWTs, which includes the material and structures. We also discuss the uncertainties within the geotechnical properties in Section 2.3, which may indirectly impact both of the structural *capacity* and *demand* of the system. Section 2.4 presents temporal uncertainty considerations and Section 2.5 discuss the modeling uncertainties. The reliability methods and examples are provided in Sections 3.1 and 3.2, respectively, where the structural capacity and demand are combined to determine the structural reliability of FOWTs.

2.1. Environmental load

The design of FOWTs must account for the various environmental loads such as aerodynamic loads on the rotor and tower, the hydrodynamic forces on the mooring system and floating platform, as well as the coupling between them. These will determine the structural demands of FOWTs. Therefore, an accurate prediction of environmental loads including various stochastic wind, wave, and current conditions is critical. This section presents extensive literature of the various research that has considered the uncertainties of the environmental loads in the development of wind turbines. The summary tables of variabilities and uncertainty models are provided over the text and discussions are placed at the end of each section.

It noted that variability and uncertainty are two distinct concepts. The term *variability* pertains to the inherent variation present within the modeled physical systems, or the environment being considered, which is described by a distributed quantity that encompasses a range of potential values. Some literature characterizes this variability as one of the *aleatory* uncertainties which are irreducible. On the other hand, the *uncertainty* represents a possible limitation in any stage or aspect of the modeling process arising from a lack of knowledge. This can typically be described in the form of a probability distribution, while there are non-probabilistic uncertainties discussed in the previous section. In this paper, the term "uncertainties" specifically refers to *epistemic* uncertainties.

2.1.1. Wind

Wind characteristics are parameters that are used to describe the wind such as wind speed and profile, turbulence intensity, dynamic wind spectrum, and wind direction. Due to interannual variability and inaccurate measurements (e.g., sensor inaccuracy, human error, and physical or atmospheric interference), wind characteristics are highly uncertain. Prior to a wind turbine project execution, details of these stochastic variables (available at the proposed site) must be obtained and analyzed for the viability/suitability of the proposed site for the turbine design and project. For the design of wind turbines, the longterm wind conditions that are dominated by the mean and standard deviation of the wind speed, serve as a representation of the wind climate. The standard deviation (σ) of annual mean wind speeds to the long-term mean value is often used to illustrate the Inter-annual variability (IAV). Therefore, it is often expressed as a percentage of the mean. The standard deviation value of IAV is typically assumed as 6% of the annual average wind speed [23,24]. This indicates that the long-term mean wind speeds annual variability at various ground sites are comparable and might reasonably be considered to be a normal distribution with $\sigma=6\%$. This assumption plays a crucial part in assessing the uncertainty in predicting the wind farm. Nevertheless, the assumption derives from examining wind speeds at 10 m above the ground level [23,25,26], employing data either from a small number of in-situ monitoring stations or from reanalysis output of a relatively coarse resolution [27]. Pryor et al. [28] developed numerical simulations using the Weather Research and Forecasting (WRF) model in order to investigate IAVs with the mean wind speed near the typical wind turbine hub height. They concluded that the annual mean wind speed variability at a height of a typical wind turbine hub in the eastern USA was less than a 6% standard deviation. Table 1 summarizes some literature data on the IAV of the wind climates.

Wind data usually consists of thousands of measurements over an extended period (e.g., 20–50 years) for the wind direction and speed. Fig. 1(a) through Fig. 1(c) represents a clustered wind direction distribution with 12, 32, and 360 direction sectors, respectively, in the north sea (80 km away from the Sylt island in Germany) for a period of 8 years (2010–2017) [31]. While increasing the number of wind sectors may enhance the accuracy of the model, it is important to exercise caution as excessive number of sectors can lead to overfitting. Fig. 2 plots the wind speed data fitted by a Weibull distribution for a wind direction sector

Table 1
Summary of the wind climates inter-annual variability [28].

Study	Descriptor	Data type	Location	No. of sites	Data duration	Assumption	Magnitude
[28]	Annual mean wind speed (m/s)	WRF output at 12 by 12 km grid cells	Eastern North America	-	15 years	Median & interquantile range	5.20% & 5.50%
[26]	•	Observations at 10 m	Ireland	-	13 years	Gaussian distribution	4.40%– 6.90%
[25]		Spatial composites of 10 m observations	UK	-	29 years	Gaussian distribution	3.10%– 7.00%
[29]		NARR interpolated to 80 m	-	-	36 years	Max %increase or %decrease in wind speed anomaly from 35-year mean	5.00%– 40.0%
[30]		Observations at 10 m	Scotland	-	13–43 years	Dispersion is divided by mean from one year to the next year	10.0%– 15.0%
[27]		Reanalysis	-	-	41 years	Gaussian distribution	8.00%– 12.0%
[23]		Observations at 10 m	=	30	_	Gaussian distribution	~6.00%

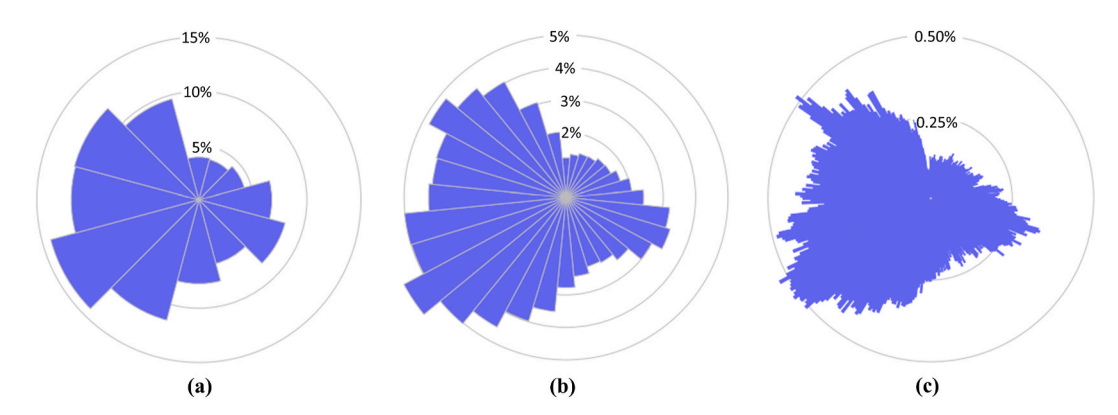


Fig. 1. Wind direction measurements at a 100 m height in the North Sea between 2010 and 2018 clustered in wind direction sectors of (a) 12, (b) 32, and (c) 360 [31].

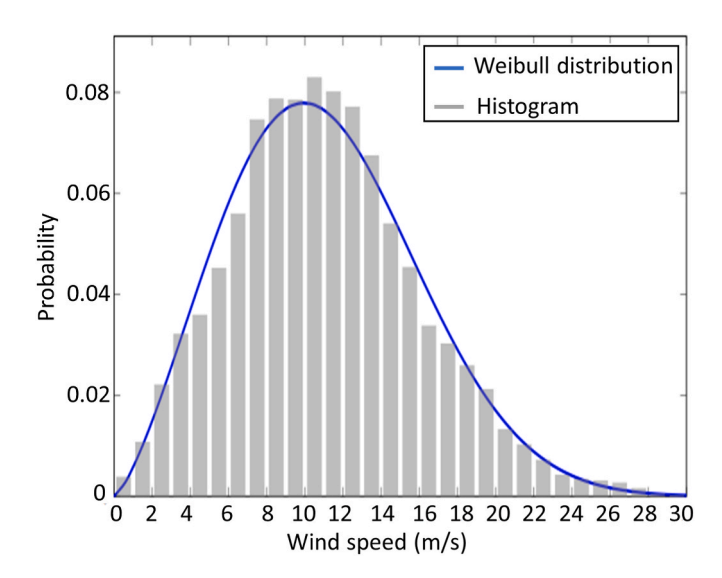


Fig. 2. Wind direction Weibull distribution in the North Sea between 2010 and 2018 for the wind direction sector [225°, 255°) facing southwest [31].

between 225 °-255 ° using the maximum likelihood estimation method [31]. To simulate a wind farm, every sector of the wind direction and the corresponding wind speed should be taken into account. It is worth noting that in an offshore wind farm, the upstream turbines decelerate the incoming wind flow (because of the viscous interaction along the blades) and the wake effect is generated which is responsible for the wind speed reduction for the subsequent FOWTs. Various models have been constructed to consider the wake effect including the Park wake

model, linearized Reynolds-average Navier-Stokes model, Eddy-viscosity wake model, large Eddy simulations, and deep-array wake model [32–36].

Different probability distribution functions (PDFs) were used in the literature to fit the wind speed data. Ouarda et al. [37] investigated the suitability of one-component parametric distributions. They concluded that Generalized Gamma and Kappa distribution functions provided the best fit for estimating the wind speed among others. Previous research exhibited that Weibull distribution might be utilized to adequately represent the wind speed probability distribution for wind energy forecasting. International Electrotechnical Commission (IEC) [38] suggested using Rayleigh distribution for predicting wind speed data analysis and annual energy production. Rayleigh distribution is a two-parameter (2-p) Weibull distribution with the shape factor (κ) of 2. However, Rayleigh distribution may lead to incorrect results [39]. Table 2 summarizes wind component's variability along with the most widely used distributions which include two- or three-parameter distribution functions in the literature. It is noteworthy to acknowledge that various studies utilized different equations and methods to derive the parameters indicated as P1 to P3 in Table 2. For instance, in Refs. [40,41], the 2-parameter Weibull distribution parameters were obtained through distinct approaches. In Ref. [40], the Method of Moments was employed, while the empirical method of Lysen was utilized in Ref. [41]. For comparison purposes, in addition to data related to offshore wind turbines (herein, shallow-water for depths less than 60 m [40,42-50] and deep-water for depths greater than 60 m [14,48,51-59]), onshore wind turbine data is also included [37,40,41,48,60-67]. In order to facilitate a direct comparison Fig. 3(a) shows the boxplots of the mean wind speed at a height of 10 m (as indicated in the last column of Table 2) for deep-water, shallow-water, and on-shore wind turbines. To achieve this comparison, it is necessary to extrapolate the mean wind

 Table 2

 Uncertainty models of wind characteristics in literature.

tudy	Variable	Original data							Mean wind speed a
		Distribution type	P1 ^a	P2 ^b	P3 ^c	Reference height (m)	Mean at reference height	COV	10 m height (m/s)
4]	Wind speed (m/s)	Normal	12	0.6	-	90	12 & 14	0.05	8.82 & 10.29
6]		2-p Weibull	2.66	12.8	-	10	11.4	0.4	11.4
9]		2-p Weibull	2.56	11.04	-	10	9.8	0.42	9.8
		Lognormal	2.18	0.48	-	10	2.18	0.22	2.18
		Gamma	5.13	0.52	-	10	9.56	0.45	9.56
0]		2-p Weibull	1.98	2.86	-	10	2.79	0.48	2.79
			2	5.5	_	40	5.31	0.49	4.37
			2.01	6.27	_	50	6.05	0.49	4.83
			2.03	7.6	_	70	7.33	0.49	5.58
			2.04	8.25	_	80	7.96	0.49	5.95
			1.94	7.31	_	10	6.48	0.54	6.48
			2.17	9.19	_	40	8.14	0.49	6.70
			2.22	9.56	_	55	8.47	0.48	6.67
			2.24	9.66	_	70	8.56	0.48	6.52
			2.27	10.16	_	80	9	0.47	6.73
1]		2-p Weibull	-2.05	3.18	_	20	2.81	0.52	2.55
11		2-p Weibun	2.10	3.77	_	40	3.34	0.52	2.75
			2.11	4.16	_	60	3.73	0.5	2.90
_		O m 147a:111	2.11	4.47	-	80	3.96	0.5	2.96
5, 46]		3-p Weibull	9.49	2.19	2.28	100	_	_	_
i7]		_	-	-	-	90	49	-	36.02
			-	_	-	90	23.2	_	17.06
53]		Generalized Extreme	-	_	-	10	8.23	0.44	8.23
		Value (GEV)	-	-	-	10	7.62	0.46	7.62
			_	_	-	10	8.28	0.46	8.28
			_	-	-	10	7.14	0.45	7.14
1]		2-p Weibull	_	_	_	10	11.4	_	11.4
			_	_	_	10	21	_	21
8]		2-p Weibull	2.36	6.7	_	10	5.91	0.48	5.91
		•	2.49	7.81	_	10	6.94	0.43	6.94
			2.45	8.09	_	10	7.18	0.43	7.18
7]		3-p Weibull	2.097	5.104	-1.269	10	4.59	0.51	4.59
		2-p Weibull	1.655	4.195	_	10	3.71	0.63	3.71
3]		2-p Weibull	2.5	1.495	_	10	1.32	0.43	1.32
[3]		3-p Weibull	3.499	1.969	- -0.438	10	1.32	0.43	1.32
		Gamma	3.941	0.338	-0.438	10	1.29	0.52	1.29
									2.18
.01		Lognormal	0.153	0.592	-	10	2.18	0.48	
[8]		2-p Weibull	2.12	9.77	_	90	8.64	0.5	6.35
			2.13	9.5	-	90	8.41	0.49	6.18
			2.1	8.38	_	90	7.42	0.5	5.45
7]		Gamma	-	-	-	10	2.47–4.28	0.53-0.70	2.47-4.28
			-	-	-	30	3.85	0.52	3.30
			-	-	-	40	4.06–5.61	0.47 - 0.50	3.34-4.62
			_	-	-	50	4.37	0.49	3.49
			-	-	-	60	5.67	0.48	4.41
			-	-	-	80	5.8	0.46	4.33
[4]		Maximum Entropy	1.98	9.12	0.9	10	32.02	_	32.02
7]		2-p Weibull	1.94	6.89	-	80	6.11	0.52	4.57
			2	5.35	-	80	4.75	0.53	3.55
			2.11	6.33	-	80	5.61	0.5	4.19
9]		2-p Weibull	1.92	8.03	_	97.35	7.12	0.55	5.18
			1.94	6.86	_	26.31	6.08	0.54	5.31
0]		2-p Weibull	1.08	1.80	_	10	2.32	0.76	2.32
-		•	1.11	1.82	_	10	2.51	0.76	2.51
			0.98	1.23	_	10	1.78	0.764	1.78
			0.96	1.57	_	10	2.18	0.90	2.18
5]		Lognormal	2.8	0.16	_	10	16.71	0.16	16.71
			2.79	0.17	_	10	16.6	0.17	16.6
			2.79	0.16	_	10	16.42	0.17	16.42
4]		2-p Weibull	1.94	8.56	_	10	7.57	0.16	7.57
-73		7-h Meinnii							
			2.12	7.77	_	10	6.88	0.496	6.88
-1		0 - 147-11 11	1.74	8.29	-	10	7.39	0.593	7.39
5]		2-p Weibull	3.05	11.13	-	10 (Site A)	9.94	0.358	9.94
			2.58	9.21	-		8.18	0.416	8.18
			2.27	7.53	-		6.67	0.467	6.67
			6.62	11.415	_	10 (Site B)	10.65	0.177	10.65
			3.85	9.895	-		11.06	0.29	11.06
			2.665	7.851	_		6.98	0.4	6.98
			2.000						
6]		2-p Weibull	2.02	4.81	_	10	4.243	0.53	4.243
66] 62]		2-p Weibull 2-p Weibull			_	10 10	4.243 2.7	0.53 0.42	4.243 2.7

(continued on next page)

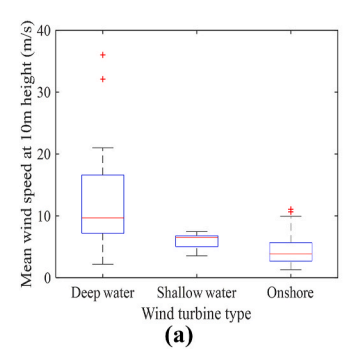
Table 2 (continued)

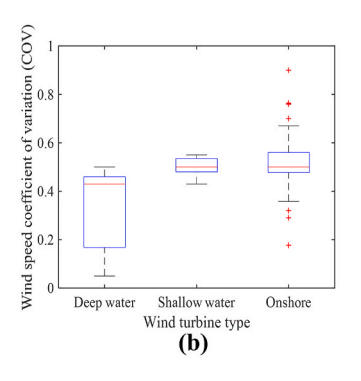
Study	Variable	Original data							Mean wind speed at
		Distribution type	P1 ^a	P2 ^b	P3 ^c	Reference height (m)	Mean at reference height	COV	10 m height (m/s)
			2.04	11.68	-	83.9	10.05	-	7.46
[45,	Wind direction	Von Mises Mixture	0.277	1.02	111	100	-	-	-
46]	(°)		0.433	2.02	227	100	-	-	_
			0.29	1.73	324	100	-	-	-
[58]			-	[-0.5:0.12]	0.38-2.62	90	-	-	_
			-	[-0.42:0.27]	0.66–88	90	-	-	_
			_	[-0.02:0.38]	1.08-3.22	90	-	-	_
[61]			0.106	2.796	-	10 (Site A)	41.94	-	_
			0.577	12.067	-		83.37	-	-
			0.189	1.034	_		223.0	-	_
			0.074	30.464	-		249.4	-	-
			0.359	7.406	_		67.72	-	_
			0.510	40.284	-		76.03	-	_
			0.079	5.106	-		170.2	-	_
			0.029	5.269	-		266.1	-	_
			0.024	16.656	-	10 (Cit. D)	359.3	_	_
			0.366	7.817	-	10 (Site B)	0.000	-	_
			0.209	51.813	-		20.46	-	_
			0.086	53.947	_		43.43	-	_
			0.059	4.928	_		74.43	-	_
			0.149	3.386	-		201.2	-	_
			0.097	14.489	_		292.8	-	_
			0.860	34.416	-		17.13	-	_
			0.045	144.385	_		42.80	-	_
			0.027	3.002	-		57.52	-	_
			0.013	44.976	_		176.5	-	_
[[0]	Thurst found	Turno Normal	0.055	1.163	_	70.15 (from	325.0	- 0.1	_
[52]	Thrust force (MN)	Trunc. Normal	781 (static)	78.1 (static)	_	70.15 (from mudline)	781	0.1	-
			197 (fatigue)	39.4 (fatigue)	_		197	0.2	_
[57]		-	-	-	-	-	173	0.37	_
[44]		Normal	0.129	0.028	-	17.73 (from mudline)	0.13	0.22	-
[68]	Wind Pressure (kPa)	Gumbel	-	-	-	At rotor height	538	0.23	-
[42]	Turbulence	Weibull & Gamma	_	_	_	10	29.2 (for 2 m/s)	_	_
	Intensity (%)		_	_	_	10	20.4 (for 4 m/s)	_	_
	, , ,		_	_	_	10	17.5 (for 6 m/s)	_	_
			_	_	_	10	16 (for 8 m/s)	_	_
			_	_	_	10	15.2 (for 10 m/	_	_
			_	_	_	10	s) 14.6 (for 12 m/	_	_
							s)		
			-	-	-	10	14.2 (for 14 m/s)	_	-
			-	-	-	10	13.9 (for 16 m/ s)	_	_
			-	-	-	10	13.6 (for 18 m/ s)	-	_
			-	-	-	10	13.4 (for 20 m/s)	-	-
			-	-	-	10	13.3 (for 22 m/	-	_
			-	-	-	10	s) 13.1 (for 24 m/	-	-
			_	_	_	10	s) 13.0 (for 26 m/	_	_
							s)		
[50]		3-p Weibull	0.009 0.01	0.134 0.14	0.534 0.484	90 90	18 (for 16 m/s) 12.4 (for 20 m/	0.18 0.124	
			0.009	0.141	0.565	90	s) 14.4 (for 20 m/	0.144	_
			0.01	0.139	0.638	90	s) 16.5 (for 20 m/		
							s)	0.165	-
			0.009	0.145	0.59	90	12 (for 24 m/s)	0.12	_
[68]		Lognormal	_	_	-	Rotor height	5	0.05	_

^a Parameter 1: shape factor for Weibull distribution, mean for Lognormal distribution, shape parameter for Gamma distribution, weight parameter for Von Mises

b Parameter 2: scale factor for Weibull distribution, standard deviation for Lognormal distribution, rate parameter for Gamma distribution, concentration parameter for Von Mises distribution.

^c Parameter 3: displacement factor in 3-p Weibull distribution.





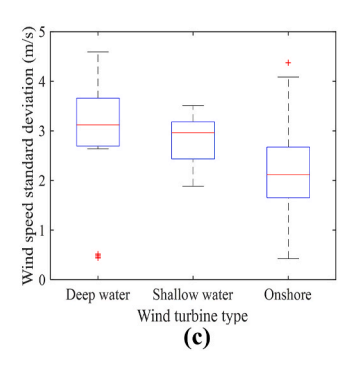


Fig. 3. Boxplots for different wind turbine types: (a) mean wind speed, (b) mean wind speed coefficient of variation, (c) mean wind speed standard deviation.

speeds measured at different heights in various studies to a consistent height (herein, 10 m). This extrapolation was accomplished using the following well-established equation [38]:

$$v_z = v_{z_0} \times \left(\frac{z}{z_0}\right)^a \tag{1}$$

where v_z represents the mean wind speed at various reference heights, v_{z_0} is the mean wind speed at the height of $z_0 = 10$ m, and α is the wind shear exponent which is commonly accepted as 0.14 [42,43]. The boxplots show minimum and maximum values, first and third quartiles, medians, and outliers. It is noteworthy to mention that the exceptionally high mean wind speed of 36.0 m/s pertains to storm conditions, specifically followed by the responses to 50-year extreme values according to the IEC design standards, North Sea statistics, and Portugal's coastal storm data [57]. Fig. 3(b) and (c) show the boxplots of the coefficients of variations (COV; the ratio of the standard deviation to the mean value) and standard deviation of the mean wind speed data, respectively. The median, minimum and maximum, and first and third quartiles of the wind speed COV at deep water exhibited lower values than both shallow water and onshore wind turbines, while the standard deviation values exhibit different trends. Overall, Fig. 3 indicates stronger and steadier winds as turbines are placed farther from the shore.

Through extensive literature data analysis, it is found that the 2-p Weibull distribution is the most prevalent distribution function for estimating wind speed [62,66,67]. Nevertheless, in meteorological conditions that provide high percentages of null wind speed, a 3-p Weibull distribution function is recommended over a 2-p Weibull distribution in general engineering practices in the industry. The suitability of a 3-p Weibull distribution and its preference over a 2-p Weibull distribution was also outlined by several studies [69,70].

The most common methods for determining the Weibull parameters include the maximum likelihood method (MLM), graphical method (GM), and least square method (LSM). Yaniktepe et al. [60] studied the wind properties and potential energy production in Osmaniye (east of the Mediterranean Sea), Turkey. They employed Rayleigh and 2-p Weibull distributions for 44 months wind speed data collected fro 2008 to 2011. The graphical method was used for determining the Weibull parameters (k and c). Altunkaynak et al. [64] employed perturbation theory to formulate wind power expectations and statistical parameters (coefficient of variation and standard deviation), which followed a Weibull distribution. Keyhani et al. [66] assessed the potential of wind energy using the wind speed statistical data in Tehran, Iran, for a period of eleven years (1995-2005). Weibull shape and scale parameters were obtained on a yearly basis. Other techniques for estimating Weibull parameters were also compared for the wind data in Brazil and Pakistan [41,65]. Costa Rocha et al. [65] used the wind speed data of two cities in the northeast of Brazil from 2004 to 2006 in order to assess the effectiveness of seven numerical techniques in determining Weibull parameters: 1) maximum likelihood method (MLM), 2) modified maximum likelihood method (MMLM), 3) graphical method (GM),

4) moment method (MM), 5) energy pattern factor method (EPFM), 6) equivalent energy method (EEM), and 7) empirical method (EM). They concluded that the EEM was the most efficient method, while GM and EPFM were the least efficient techniques for fitting the wind speed data using Weibull distribution. In another study, Saeed et al. [41] used two years (2016–2018) of wind speed data at four different heights from sea level to assess the wind energy potential in North of Pakistan. Six numerical methods including Empirical method of Justus (EMJ), Empirical method of Lysen (EML), modified maximum likelihood method (MMLM), Graphical method (GM), Method of Moments (MoM), and Energy pattern factor method (EPFM) were used for determining the Weibull parameters. Among these methods, MMLM was the most efficient technique, while the GM was the least effective to fit the wind data. In another comprehensive study, the 2-p Weibull distribution exhibited the best fit, performing better than some of the 3-p distribution functions such as the 3-p Lognormal and the Generalized Extreme Value [37]. On the other hand, Pobocikova et al. [63] reported that 3-p Weibull distribution fits the wind speed data best, and 2-p Weibull distribution is the second best distribution function compared to the 2-p Gamma and 2-p Lognormal distributions.

The standard deviation of turbulence intensity significantly affects the wind excitation spectrum more than the horizontal average wind speed does. Therefore, when evaluating the safety of FOWTs under horizontal random excitation, the standard deviation of turbulence intensity must be considered. To obtain the wind load distribution, design wind, and turbulence intensity were used and a 1-h thrust force to the hub was estimated [44]. The Kaimal spectrum was used to find the turbulent wind. Horn and Jensen [71] considered the wind component's phase angle as a stochastic variable with a normal distribution. To reduce the computational burden, the environmental contour method is widely used for long-term design loads of FOWT [72,73]. To this end, the marginal distribution of the environment is required to construct the environmental contour. While this study acknowledges the existence of numerous contour methods, it is beyond the scope of the current work to provide an in-depth analysis of these techniques. For a comprehensive understanding and thorough comparisons of various environmental contour techniques, Haselsteiner et al. [74] offers a detailed examination, providing valuable insights and analyses. Li and Zhang [59] compared the three most prevalent parametric distributions for environmental parameters (Gamma, Lognormal, and Weibull distributions). They used MLE to obtain the distribution parameters, where the best fit was recognized by having the highest log-likelihood value. They reported that the Weibull distribution with the largest log-likelihood value was suitable for wind speed [59]. In a study conducted by Carta et al. [61] data on wind direction from several stations in the Canary Islands (Spain) was used. The distribution of directional wind speed was represented by a finite mixture of Von Mises probability density function. They suggested using a mixture of two Von Mises probability functions for the Canary Islands. The authors found that the maximum number (N) of probability densities exceeding 6 exhibited a dramatic decrease in the suitability of the distribution function.

In general, the wind speeds, directions, and turbulence intensities are found to be inherent uncertainties that significantly impact the reliability of FOWT structures. The uncertainty models representing these parameters in Table 2 present the COV level between 0.2 and 0.7 with a median of 0.43 for the wind speed in deep water, and COV between 0.2 and 0.4 with a median of 0.24 in shallow water. The most of literature provides 2-p & 3-p Weibull distribution as the best representation of the model based on the data. However, in the stage of reliability analyses of FOWT, it is also recommended to use the Lognormal distribution due to its simplicity. The wind direction can be considered as a variability instead of an uncertainty. Therefore, it is reasonable that COVs are not reported as commonly as wind speed. However, if uncertainties are to be modeled, one can also refer to an industrial standard where $\pm 15^{\circ}$ of variation is recommended to consider based on the given direction [75]. The turbulence intensities can be considered as variability or uncertainties depending on the purpose of the study.

2.1.2. Wave

Although both FOWTs and fixed-type OWTs are subject to significant wave-induced motions, the non-stationary structural properties of FOWTs are largely affected by the uncertainties of the wave excitations. The undulatory phenomena of wind-induced waves disturb the surface of the sea. They are produced by wind friction at the sea-atmosphere interface (wind sea) and spread over long distances (swell) by being transformed through various mechanisms. These transformations in deep water are due to the white capping and viscosity effect of energy dissipation, wind energy addition, and energy transmission to short frequencies. Therefore, wind growth, white capping, and quadruplets are the most dominant processes. Waves with small amplitudes of deep water can be expressed relatively simply and accurately at the sea surface height or elevation. The wave's field is better described by the sea state using statistical parameters such as peak period, peak enhancement factor, and significant wave height. The parameters of the model for wind sea waves (young waves) are dependent on the wind speed duration, wind speed phasing, and fetch length. Also, it is recommended that a normal distribution could be used to describe the relative direction between the young waves and wind [14,46].

The uncertainties in hydrodynamic parameters (e.g., drag coefficient) associated with wave modeling make it difficult to accurately predict the response of FOWTs. Taylor et al. [19] and Ruzzo et al. [76] introduced constrained quasi-deterministic wave models to consider the random nature of the oceanic waves. To predict the hydrodynamic loads due to waves and floater motions, a hybrid analysis method is widely used which is combining 3D diffraction/radiation theory and the semi-empirical formula Morison equation [77,78]. For diffraction dominant floating structure members, hydrodynamic loads such as radiation damping, added mass, quadratic sum and difference wave force transfer function (QTFs), and linear wave force transfer function (LTFs) are estimated by using 3D diffraction/radiation theory, and viscous loads are obtained using the Morison equation. On the other hand, hydrodynamic forces on the slender members of a floating structure are estimated by the Morison equation.

In the Morison equation, hydrodynamic forces consist of two components: drag force (FD) which is attributed to the inertia force (FI), and water particle velocity as a result of the water particle acceleration. The drag coefficient in the Morison equation is characterized by the Keulegan-Carpenter (K–C) number and Reynolds number. In general engineering practices in the industry, a constant drag coefficient is used for the analysis. Therefore, there are limitations to analyzing drag loading in random sea states. According to previous research [79–82], uncertainties inherent in Morison's equation are crucially important and cannot be neglected. In addition, 3D diffraction theory has been developed up to 2nd-order accuracy. To overcome theoretical limitations, Computational Fluid Dynamics (CFD) simulations and scaled model tests are widely used for extracting highly non-linear hydrodynamic loads. However, CFD simulations are still too expensive to replace the

conventional design analysis tools, and the scaled model tests have inherent scale effects. Therefore, there are uncertainties and limitations in calculating highly non-linear waves and motions-induced loading on the floating structure.

Some researchers recommended environmental parameters like peak period and significant wave height with their relevant probability distribution to be considered for the reliability analysis of FOWT [11,45,59]. Also, the influence of wave load on the reliability assessment of wind turbines with appropriate distribution and limit state functions has been taken into account as stochastic parameters in the design process [44,52]. The wave uncertainty can also be expressed as a distribution combined with Lognormal and Weibull distributions [83] for fatigue evaluation. To limit the number of random variables in an irregular sea, wave amplitudes can often be defined as a deterministic variable [71], while it can also be modeled as a random variable with Rayleigh distribution. The phase angles can be modeled with uniform or normal distribution. Table 3 summarizes wave component variabilities.

In addition, the presence of abnormal waves, such as solitary waves, freak waves, and wave groups, poses significant challenges for FOWTs [89,90]. These waves can lead to structural damage, reduced operational lifespan, and increased fatigue. Advanced modeling and forecasting systems are being developed to better understand and predict these waves, enabling engineers to enhance turbine design and operational strategies. Ongoing research focuses on improving turbine survivability through optimized structural design, adaptive control systems, and real-time monitoring [91–93]. Mitigating uncertainties related to abnormal waves enhances turbine performance, safety, and the growth of offshore wind energy.

The responses of FOWTs cannot be estimated by a single met-ocean parameter. Consequently, various models have been proposed to fit the joint distribution of significant wave height (H_s) and conditional mean period (T_{02}). For accurate estimation of the long-term probability of sea state occurrences, it is critical to have a continuous dataset and fit it with an appropriate probabilistic model. Typically, joint probability theorem is employed for the conditional modeling using Eq. (2).

$$f(H_s, T_{02}) = f(H_s) \times f(T_{02}|H_s)$$
 (2)

where $f(H_s)$ is the marginal distribution of significant wave height, $f(T_{02}|H_s)$ is the distribution of the mean zero-crossing period conditional on significant wave height, and $f(H_s, T_{02})$ denotes the joint PDF of the mean wave period and significant wave height. The joint distribution in Eq. (2) can be obtained using both peak and mean wave periods. It should be noted that wind-wave parameter correlations play a key role in determining the joint probability distribution. A multivariate distribution or copula function can be used for the joint modeling of wave parameters and wind speed to capture their correlations [94,95]. By incorporating wind speed into the conditional modeling, $f(H_s, T_{02})$ can be expanded to a multivariate distribution by introducing wind speed as an additional variable. The Weibull distribution function is employed to fit the marginal significant wave height data [11,96–100]. The accuracy of the extrapolated wave height using the environmental contour method is dependent on the quality and length of the data. When using calibrated hindcast predictive models, the statistical, model, and measurement errors introduce uncertainties within the design conditions [101]. The wave period is often modeled using the Lognormal distribution function. The mean (μ) and standard deviation (σ) of the Lognormal distribution are employed for wave period prediction and is formulated in Eq. (3) and Eq. (4), respectively [11].

$$\mu_t(H_s) = a_1 + a_2 H_s^{a_3} \tag{3}$$

$$\sigma_t(H_s) = b_1 + b_2 e^{b_3 H_s} \tag{4}$$

FOWTs' heave natural period is in the wave frequency range, which is influenced by the uncertainties in the wave-breaking phenomenon. The wave-breaking limit depends on the physical and environmental

Table 3Uncertainty models for wave properties at both shallow and deep-water sites.

Study	Variable	Distribution	P1 ^a	P2 ^b	P3 ^c	Mean	COV
[14] ^d	Significant wave height (m)	Normal	8.52	0.43	-	8.52	0.05
[84]		3-p Weibull	2.26	2.77	0.03	2.44	0.47
[59] ^d		Gamma	5.54	1.8	-	3.08	0.24
		2-p Weibull	2.47	3.48	_	3.09	0.43
		Lognormal	_	_	_	1.03	0.43
[45,46]		3-p Weibull	1.56	1.43	-0.09	-	-
		3-p Weibull	0.64	1.32	0.33	-	-
[51]		Gumbel	_	_	_	15.6	_
			-	-	-	9.5	-
[85]		Normal	2	0.25	_	2	0.13
[86] ^d		3-p Weibull	1.46	0.87	0.26	1.04	0.57
		Lognormal	-0.09	0.49	-	1.04	0.57
[87] ^d		Lognormal	-	-	_	3.48	0.59
[88]		3-p Weibull	0.89	1.47	2.77	_	_
[55] ^d		3-p Weibull	1.47	2.46	4	6.23	0.25
		-	1.42	2.36	4	6.15	0.25
			1.21	2.08	4	5.95	0.27
[83]		2-p Weibull	_	_	_	2.7	0.26
		-	_	_	_	2.7	0.1
			_	_	_	2.7	0.08
[83]		2-p Weibull	2	4.58	_	4.06	0.53
		-	1.25	2.03	_	1.9	0.8
[14] ^d	Wave period (s)	Normal	12.45	0.62	-	12.5	0.05
[84]		Lognormal	2.07	0.39	-	2.07	0.19
[59] ^d		Lognormal	2.37	0.24	-	2.37	0.1
		Gamma	18.4	1.68	_	10.9	0.23
		2-p Weibull	4.34	11.93	-	10.9	0.26
[45,46]		Lognormal	-	-	-	1.61	0.22
[51]		Lognormal	-	-	-	2.03	0.14
		Gumbel	-	-	-	11.06	-
			-	-	-	6.93	-
[58]		Gamma	0.63-167	0.03-0.30	-	21-556.6	0.07
			0.78-126	0.04-0.52	-	19.5-242	0.09
			1.22-116	0.03-0.16	-	40.6-725	0.09
[86] ^d		Lognormal	1.69	0.19	-	5.53	0.2
		3-p Weibull	2.51	2.9	2.96	5.53	0.2
[87] ^d		Lognormal	-	-	-	10.5	0.24
[88]		Lognormal	2.26	0.54	-	2.54	0.05
[55]d		Lognormal	11.5	1.37	-	11.5	0.12
			11.5	1.26	-	11.5	0.11
			11.2	1.34	-	11.2	0.12
[83]		Lognormal	21.7	-	-	21.7	N/A
			5.81	-	-	5.81	N/A
[45,46]	Relative wave-wind direction	Trunc. Normal	-	-	-	0.24	71.8
[85]	Mean sea level (m)	Normal	31	3.5	-	31	0.11

^a Parameter 1: shape factor for Weibull distribution, mean for Lognormal distribution, shape parameter for Gamma distribution, α parameter for Maximum entropy distribution.

characteristics [101]. Raed et al. [11] estimated the uncertainties of a semi-submersible platform, compatible with the environmental condition of the northern part of the North Sea. Log-normal and Weibull distributions were used to fit the recommended conditional distribution of the mean zero up-crossing period and the marginal distribution of the significant wave height [88]. They employed an alternative approach utilizing Monte Carlo simulations of the joint environmental model for establishing the environmental contour lines in the original space [88]. The 3-parameter Weibull and Lognormal distributions were used to model the marginal significant wave height and the conditional distribution of the mean wave period, respectively. Although the proposed method produced similar findings as conventional inverse first-order reliability method (IFORM), it arguably had two advantages: 1) resulting contours allowed for easier interpretation in the original space, and 2) the proposed approach did not require a joint parametric model to account for the environmental parameters.

Dong et al. [87] employed bivariate Maximum Entropy (ME) distribution for both significant wave height and corresponding peak period. According to the maximum entropy theory, over the set of probability distributions, the probability model that maximizes entropy is the best for describing data [102]. It is the most unbiased estimate based on the available information and is as noncommittal as possible regarding missing information. Maximum Entropy distribution can be used to predict the marginal PDF of the significant wave height.

In general, the uncertainties of the significant wave heights and the periods are identified as those impacts the structural reliability of FOWTs. The most typical probability distribution for the significant wave height is found to be Weibull distribution. In addition, other distributions such as Lognormal and Gumbel distributions are used. For the simplicity of the structural reliability calculation of FOWTs, we identified Lognormal distribution as a practical option. The COV levels between 0.1 and 0.5 are found with a median of 0.2, i.e., 20% of the

 $^{^{}b}$ Parameter 2: scale factor for Weibull distribution, standard deviation for Lognormal distribution, rate parameter for Gamma distribution, β parameter for Maximum entropy distribution.

 $^{^{\}rm c}$ Parameter 3: displacement factor in 3-p Weibull distribution and ζ parameter for Maximum entropy distribution.

^d Correlation between wind and significant wave height was studied.

uncertainties. Similarly, the median value of the uncertainties in the wave periods is estimated to be approximately 15%.

2.1.3. Current

The movement of water from one location to another is referred to as an oceanic current. Tidal currents are caused by astronomical forces and coexist with the tide's rise and fall in the sea level. The direct impact of the wind's shear stress on the water's surface produces wind-generated currents which are typically found in the upper layer of a body of water. The mean speed of a typical ocean current ranges from 0.2 m/s to 0.6 m/ s, and the maximum speed ranges between 1.1 m/s and 2.7 m/s, depending on the location of the site [103]. Currents would add viscous loads on FOWTs. In addition, the presence of current affects the wave loads through the transformation of the wave shapes due to the wave-current interactions [104]. The wave-current interactions might change the FOWTs responses, and therefore must be considered. When the directions of the current and wave are opposite, the wavelength becomes shorter, and the wave height increases, leading to the formation of steeper waves [104]. The wave height could occasionally reach more than 30 m in height, which can severely damage FOWTs [90]. Conversely, when current and wave follow the same direction, wavelength becomes longer and wave height reduces, resulting in the formation of shallower waves. Qu et al. [90] studied the impact of wave-current interaction on the dynamic responses of a Spar-type FOWT, called the doppler effect. They reported that the opposite current increased and the following current decreased the peak value of the wave spectrum. However, the met-ocean data delivered to the designer already includes the interaction effects as the instruments cannot measure current and wave separately.

Like wind speed, the current speed also fluctuates in space and time. The timescale and length of current speed variations, however, are much greater than that of the wind speed [105]. Thus, currents might be characterized as a function of the vertical coordinate in space and a constant velocity in time [106]. Fig. 4(a) illustrates the recorded ocean current speed measurements obtained from the Su-ao anchor station in Taiwan, specifically at a depth of 30 m below sea level [107]. To distinguish between sub-surface and near-surface components of the currents, the measured values of current speed and direction may be converted as follows [38]:

$$v_{z,SS} = v_{0m,SS} \left(\frac{d-z}{z}\right)^{1/7}$$
 (5)

$$v_{z,NS} = \begin{cases} v_{0m,NS} \left(\frac{20m - z}{20m} \right) & \text{for } z \le 0 \\ 0 & \text{for } z > 0 \end{cases}$$
 (6)

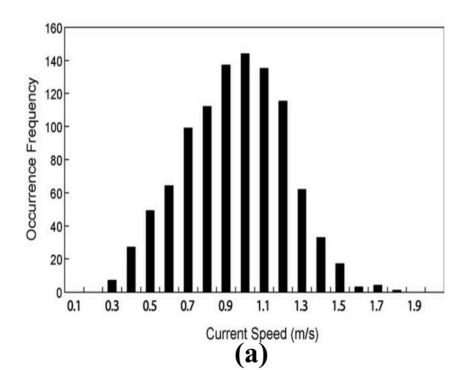
where $v_{z,SS}$ and $v_{z,NS}$ denote sub-surface and near-surface current speeds at a position of z below sea level, and d represents the ocean depth. In the study conducted by Hübler et al. [42], sub-surface and near-surface

current speed profiles were plotted using Eq. (5) and Eq. (6). These profiles were specifically generated for a water depth of 25 m, with the normalization of current speeds (i.e., $v_{0m,SS} = v_{0m,NS} = 1$), as depicted in Fig. 4(b).

In order to better understand the hydrodynamic performances of FOWTs, particularly the interaction of wave-current-structure, a moored platform in regular wave and uniform current was taken into consideration [108]. It was found that the current had considerable effects on low-frequency motions and the mean wave-drift forces. Most direct time-domain second-order models disregard the effects of forward speed or current. Nevertheless, the offshore sites' current speeds might be non-negligible, particularly in FOWT applications with small cross-section dimensions. Hydrodynamic forces caused by waves and currents, such as viscous force and inertia, are critical in the design of FOWTs, and dynamic response evaluations are necessary for the specific design of load cases in accordance with design standards and recommendations to ensure that FOWTs have sufficient stability and structural strength [109]. Therefore, the safety of mooring lines relies on an accurate estimate of the current load on the floating platform. To model the nonlinear random wave groups with a superimposed current. Nava et al. [89] developed a second-order quasi-deterministic theory. Ou et al. [90] developed a more effective phase modulation algorithm considering the randomness of the wave groups with high efficiency. They then analyzed the effect of current on the wave energy spectrum taking into account various current velocities for determining the dynamic responses of a spar-type FOWT. Their analysis provided insights into the wave-current interaction mechanism for identifying extreme wave conditions in Gaussian seas which is critical for the analysis for the design of FOWTs.

2.1.4. Correlation between the environmental loads

The current practices (e.g., IEC 61400-3 [110]) necessitates the utilization of joint wind speed and wave height distributions, rather than independent sets of wind and wave information. Generally, the sets of waves are calculated from wind information prior to the analysis. For instance, significant wave height and period at the peak of the spectrum of a fully developed sea were estimated using the Pierson-Moskowitz spectrum [111] or JONSWAP (Joint North Sea Wave Observation Project) spectrum [112]. Since the correlation between the environmental loads may significantly affect the results, the proper correlation needs to be modeled in the estimation of reliability. The correlation between the wind and wave loads and other random variables will be modeled in this task to be used in the reliability analysis. To investigate this correlation, we suggest utilizing the sets of long-term global wind/wave databases such as a) Buoy data sets from National Data Buoy Center, National Oceanic and Atmospheric Administration (NOAA), National Weather Service (NWS), b) Model data sets from National Centers for Environmental Prediction (NCEP), NOAA, Environmental Modeling Center, and c) NCEP Climate Forecast System Reanalysis Reforecast (CFSRR) 30-year homogeneous data set.



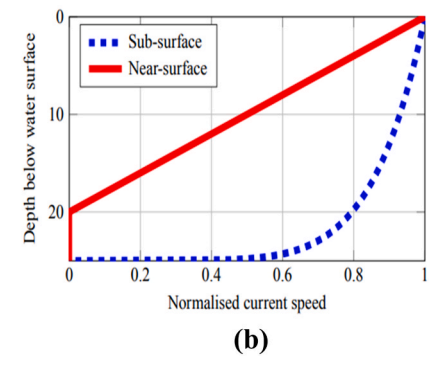


Fig. 4. (a) Sample sub-surface current speed distribution in Taiwan, (b) sub-surface and near-surface current speed profiles in the North Sea [42,107].

The intricate interaction between the environmental loads makes predicting the dynamic response of FOWT challenging. The simulation length of fixed-type and land-based wind turbines is 10 min as specified by the design standard IEC 61400-3 [110]. However, a 10-min simulation length is too short to capture extreme hydrodynamic loads on fixed-type OWTs in random sea states. Therefore, a 3-h simulation length is suggested to capture the extreme wave loads induced by random sea states. Haid et al. [113] analyzed the simulation length effect of FOWT using the nonlinear aero-hydro-servo-elastic simulation tool (FAST: Fatigue, Aerodynamics, Structures, and Turbulent). They reported that at a constant total simulation time, the length of the wind file did not affect the dependence of the aerodynamically induced load on the simulation length. The supporting platform of a FOWT must accommodate six-DOF motion because of the integrated random wind and wave loads, which complicates the random cyclic loads acting on the structural components (e.g., the tower base) compared to fixed-type or onshore wind turbines. These cyclic loads might lead to unanticipated fatigue damage to a FOWT. According to the research conducted by Chen and Basu [114], FOWT tower and cable responses are significantly affected by the current and wave-current interactions. The wave-current interaction is expected to have a more significant effect in nonlinear waves of large amplitude. Joint wind and wave distribution must be estimated prior to obtaining accurate fatigue damage in real environmental situations. The marginal PDF of the mean wind speed which follows a 2-p Weibull distribution, the conditional PDF of the significant wave height, and the joint probability density function of the mean wind speed, the peak spectral period, and significant wave height have been considered [51,115,116]. Stewart et al. [58,117] conducted extensive analyses where they constructed long-term joint probability distributions using probability distribution functions. These distributions were then utilized to create three representative sites for the United States: 1) East Coast, 2) West Coast, and 3) Gulf of Mexico. By combining the respective probability distributions, they effectively captured the statistical characteristics of wind and wave conditions at specific locations. Fig. 5 presents the correlation between the mean wind speed and the significant wave height for multiple locations within the aforementioned sites. This correlation analysis provides valuable insights into the variations and patterns that exist across different geographical regions.

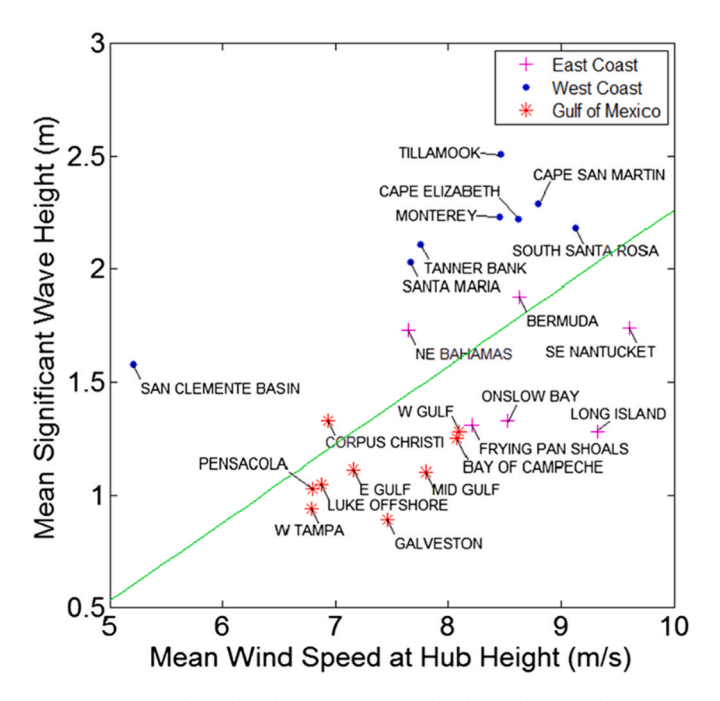


Fig. 5. Mean wind speed and significant wave height for different locations at three generic sites in the United States [58,117].

Montes et al. [55] employed Gaussian copula (Nataf model) to establish the joint probability distribution of environmental loads at three distinct sites in the Bay of Campeche located in the Gulf of Mexico. The water depth considered ranged from 500 m to 1500 m. The corresponding correlation coefficients were determined using maximum likelihood estimation (MLE). The average correlation coefficient between significant wave height and wave period was found to be 0.71 for the studied sites. Similarly, the average correlation coefficient between wind speed and significant wave height was determined to be 0.79. In contrast, the average correlation coefficient between wind speed and wave period was observed to be relatively lower, specifically 0.25.

2.2. Uncertainties within materials and structures

A FOWT structure consists of a tower, wind turbine blades, and a floating platform. The floating platform is moored to the seabed to prevent drift motions. This enables FOWTs to operate in a variety of seabed soil conditions and water depths [118]. FOWTs are subject to both hydrodynamic and aerodynamic loads. Hydrodynamic loads arise from the actions of waves, currents, and floater motions on the floating platform. Aerodynamic loads arise from the action of wind and weather on the turbine blades, nacelle, and tower. Together these loads interact with each other through the turbine tower to the floating platform connection, and through mooring connections to the foundation. This section presents the uncertainties involved in the materials and structures of these components listed above. The uncertainties presented in this section impact the uncertainties of the structural capacity and therefore on the structural reliability of FOWTs.

Based on contemporary design practices, wind turbines are generally designed for material factors that are expected to maintain target reliability levels. Traditionally, the load-carrying capacity would be calculated using deterministic equations provided in the design codes and standards. Nevertheless, significant variations in the load-bearing capacity could be observed due to the variations in the material properties [119]. Okpokparoro [14] reported that consideration of the uncertainties of material and geometric uncertainties has increased the probability of FOWT failure by up to 39%.

2.2.1. Turbine blade

Past research exhibits that the blade system's risks would result in more considerable financial losses and downtime. The blade, which has a typical slender structure, is the crucial part of the wind turbine for capturing wind energy. As the blade's length increases, the wind turbine generates more power. General Electric (GE) researchers designed the most powerful FOWT (12 MW) which was 260 m tall with a rotor diameter of 220 m. This turbine is capable of generating 67 GWh of electricity per year, enough to power 16,000 households [120]. However, under extreme environment loads, larger blades are prone to easy vibration, their anti-fatigue property would significantly reduce, and they are more likely to break [50]. Chou et al. [121] reported that the main damage types of blades under extreme environmental conditions were cracking in front/rear flanges and envelope delamination. Blades at OWTs and FOWTs are composed of Fiber Reinforced Composites (FRP). This material is usually composed of fiber and matrix materials using compounding technology. The mean stress for composite materials could significantly affect the fatigue properties [68]. Material properties are known to be the primary source of uncertainty in blade elements. Geometrical size and local defects affect the load-carrying capacity of the blade such that the weakest link model must be regarded once a small local defect appears on a blade. The variables concerned with the material and geometry (herein, thickness of the laminate) of blades are assumed to follow a normal distribution although other distribution functions including Weibull, Lognormal, etc. might also be used [68]. Gonzaga et al. [122] assumed a normal distribution for density, elastic, and shear moduli of blades in all directions. Suzuki et al. [123] proposed a novel phenomenological fatigue model

based on stiffness degradation for predicting the service life of glass fiber-reinforced plastics (GFRPs) subjected to random oceanic current loads. A Weibull cumulative density function was used to take into consideration a shift in failure modes and associated changes in the rate of damage accumulation. Also, the initial strength and the probability distributions of residual strengths were described by 3-p Weibull distributions [124].

The existing models of material uncertainties inherent in turbine blades are tabulated in Table 4. All material properties including blade thickness, density, young's modulus, shear modulus, and Poisson's ratio are assumed to follow a normal distribution.

2.2.2. Turbine tower

Similarly, the material uncertainties considered in the modeling of wind turbine tower components are represented in Table 5. Young's modulus, yield stress, and density of structural steel used in turbine towers are considered to be modeled as random variables for reliability assessment [14,52,68,130]. In the reliability analysis of FOWTs, tower failure is associated with strong winds, large waves, and typhoons [130]. Buckling is one of the limit states of offshore wind turbines resulting from the slenderness of towers [131]. The local buckling failure mode of towers was also considered by Sørensen and Toft [68]. Tower bending natural frequency changes due to the floater mass and stiffness, and rotor 3P frequency could excite the turbine's 1st bending mode which might cause fatigue damage to the blade and tower. Therefore, uncertainties in tower, blade, and floater coupled responses must be considered.

2.2.3. Mooring line

Mooring systems are sets of lines that connect the floating structure to the seabed. Mooring lines in FOWTs are used to keep the floater in a certain area (watch circle) in the presence of environmental loads. A FOWT mooring system must be designed taking into account multiple factors including the stability of an often-lightweight platform, application to relatively shallower water depths, and cost. In deep waters, the dynamic response of a floating platform withstands wave frequency forces, leaving low-frequency drift forces to be handled by the mooring system [133]. Many FOWT concepts involve light displacement platforms that are moored in shallow water and exposed to severe storms with high-speed winds. Large wind- and wave-induced motions on FOWT platforms might cause shock loadings on the mooring lines. The mooring lines' tension is closely associated with the surge, sway, and vaw motions [90]. Mooring lines are available in three distinctive geometries. Catenary, semi-taut, and taut-leg mooring lines are composed of steel cables, anchor-chains, or synthetic fiber chains and/or wire components. Table 6 summarizes uncertainty models considered in the structural reliability analysis of mooring line components in offshore wind turbines.

In summary, the material property uncertainties associated with turbine blades, towers, and mooring lines in FOWT structures exhibit varying degrees of uncertainty. Turbine blades are characterized by moderate to high levels of uncertainty, with COV values ranging from 0.02 to 0.25. Towers display moderate uncertainty, with COV values ranging from 0.05 to 0.1. Mooring lines demonstrate relatively lower to moderate levels of uncertainty, with COV values ranging from 0.02 to 0.07. Normal distribution is found to be the most widely used probability distribution for the uncertainty modeling of FOWT material properties. However, alternative distributions such as Lognormal and Gumbel distributions might also be used depending on the desired level of simplicity and accuracy in the reliability analysis.

2.3. Geotechnical Uncertainties

The foundation design of FOWTs presents some uncertainties such as scour phenomena due to the erosion of the seabed near the foundation caused by waves and currents acting together, soil-structure interaction

Table 4
Considered material and thickness uncertainties of wind turbine blades

Study	Material	Variable	Distribution	Mean	COV
122]	Bi-directional	Biaxial Young's	Normal	NP ^a	0.04
	glass fiber laminate	modulus (E ₁₁) Biaxial Young's	(Gaussian)		0.04
		modulus (E_{22}) Biaxial Young's			0.04
		modulus (E_{33})			
		Biaxial density (ρ)			0.006
		Biaxial shear modulus (G_{12})			0.03
		Biaxial shear			0.03
		modulus (G_{13}) Biaxial shear			0.03
		modulus (G_{23}) Biaxial blade			0.02
		thickness (t)			
	Unidirectional glass fiber	Uniaxial Young's			0.03
	laminate	modulus (E_{11})			
		Uniaxial Young's			0.05
		modulus (E ₂₂) Uniaxial			0.05
		Young's			0.03
		modulus (E_{33}) Uniaxial			0.006
		density (ρ) Uniaxial shear			0.03
		modulus (G12)			0.03
		Uniaxial shear modulus (G_{13})			0.03
		Uniaxial shear			0.03
		modulus (G_{23}) Uniaxial blade			0.03
125]	Unidirectional	thickness (t) E_1 (GPa)		39.04	0.0264
	(UD) layer	E_2 (GPa)		14.08	0.0231
		G ₁₂ (GPa)		4.24	0.0234
		Poisson's ratio (v_{12})		0.291	0.0934
	Structural foam	E (GPa)		75.00	0.12
		G (GPa)		20.00	0.05
		Poisson's ratio		0.42	0.1071
		(v)			
126]	Composite	Young's		45.6	0.02
	hydrokinetic material	modulus (E_{11})			
	inateriai	[GPa]		16.0	0.02
		Young's modulus (E_{22} &		16.2	0.02
		E_{33}) [GPa]			
		Shear modulus		5.83	0.02
		$(G_{12} \& G_{13})$			
		[GPa]			
		Shear modulus		5.786	0.02
		(G_{23}) [GPa]		_	
127]	E-glass fiber	Longitudinal		74	0.25
		modulus (E_{11})			
		[GPa] Transverse		74	0.20
		modulus (E ₂₂ &		<i>,</i> .	0.20
		E_{33}) [GPa]			
		In-plane shear		30.80	0.25
		modulus (G_{12})			
		[GPa]			
		Transverse		30.80	0.20
		shear modulus			
		$(G_{13 \& G_{23}})$			
		[GPa]		0.20	0.05
		Major Poisson's ratio (v_{12})		0.20	0.05
				0.23	0.044
		Minor Poisson's		0.23	0.044
	МҮ750 Ероху			0.23 3.35	0.044

(continued on next page)

Table 4 (continued)

Study	Material	Variable	Distribution	Mean	COV
		Poisson's ratio Shear modulus		0.35 1.24	0.057 0.2
[128]	E-glass/epoxy	(GPa) Density (g/	Normal	1.97	_
	laminate (unidirectional)	cm3) Longitudinal modulus (E ₁)	(Gaussian)	41	-
		[GPa] Transverse in- plane modulus		10.4	-
		(E ₂) [GPa] In-plane shear modulus (G ₁₂)		4.3	-
		[GPa] In-plane Poisson's ratio		0.28	-
		(v ₁₂) Longitudinal tensile strength (MPa)		1140	-
		Transverse tensile strength (MPa)		39	-
		Longitudinal compressive strength (MPa)		620	-
		Transverse compressive strength (MPa)		128	-
		In-plane shear strength (MPa)		89	-
	E-glass/epoxy laminate (biaxial)	Density (g/ cm3)		1.90	-
		Longitudinal modulus (E ₁) [GPa]		24.5	-
		Transverse in- plane modulus (E ₂) [GPa]		23.8	-
		In-plane shear modulus (G ₁₂) [GPa]		4.7	-
		In-plane Poisson's ratio (v ₁₂)		0.11	-
		Longitudinal tensile strength (MPa)		433	-
		Transverse tensile strength (MPa)		386	-
		Longitudinal compressive strength (MPa)		377	-
		Transverse compressive strength (MPa)		335	-
	Show about 1 form	In-plane shear strength (MPa)		84	-
	Structural foam	Density (g/ cm3)		0.25 240	-
		In-plane modulus (E ₁) [GPa]			-
		In-plane modulus (E_2) [GPa]		230	-
		In-plane shear modulus (G ₁₂) [GPa]		115	-
		Longitudinal tensile strength (MPa)		7.2	-
		Transverse tensile strength (MPa)		7.2	-

Table 4 (continued)

Study	Material	Variable	Distribution	Mean	COV
		Longitudinal		4.6	_
		compressive			
		strength (MPa)			
		Transverse		4.6	-
		compressive			
		strength (MPa)			
		In-plane shear		5.0	-
		strength (MPa)			
[129]	Various	Blade root	-	20.70	73.00
	piezoelectric	stress for			
	materials	material I			
		(MPa)		10.00	47.00
		Blade root		13.30	47.00
		stress for			
		material II			
		(MPa)		10.00	38.00
		Blade root stress for		10.60	38.00
		material II			
		(MPa)			
		Blade root		10.20	33.00
		stress for		10.20	33.00
		material VI			
		(MPa)			
		Flapwise of		1.00	2.48 ^b
		blade tip for		1.00	2.10
		material I (m)			
		Flapwise of		0.94	2.37 ^b
		blade tip for			
		material II (m)			
		Flapwise of		0.92	2.29 ^b
		blade tip for			
		material II (m)			
		Flapwise of		0.92	2.25 ^b
		blade tip for			
		material VI (m)			
		Edgewise of		0.03	0.20^{b}
		blade tip for			
		material I (m)			
		Edgewise of		0.03	0.19 ^b
		blade tip for			
		material II (m)			_
		Edgewise of		0.04	0.18 ^b
		blade tip for			
		material II (m)			
		Edgewise of		0.03	0.18 ^b
		blade tip for			
		material VI (m)			

^a Not published in the article.

(such as the interaction between mooring lines, anchors, and the seabed), soil properties, etc. The methods for soil modeling could be mainly classified into the p-y and finite element analysis (FEA) methods. The p-y method where the soil is modeled using distributed equivalent springs is widely used for reliability analysis of OWTs because of the computational efficiency. Nevertheless, the p-y method is incapable of accurately capturing the soil behavior [5]. To overcome this issue, FEA can be used to model the soil. In the FEA, the soil material is normally based on either Mohr-Coulomb or Drucker-Prager models, where the soil is generally represented using 3D brick elements. Through extensive literature data analysis on the reliability assessment of FOWTs, it was observed that soil characteristic is one of the most crucial factors considered in recent publications. Previous studies highlighted the need for additional research by investigating the impact of foundation configuration and site parameters on the natural frequency. Ziegler et al. [85] provided better insight into fatigue loads' sensitivity to varying site conditions such as soil properties. In their study, the soil was modeled using distributed linear springs via the p-y method. The soil stiffness obtained from a nominal p-y curve was scaled with a constant factor over the entire depth to represent the soil variations. Soil properties

^b Maximum values.

Table 5Considered material uncertainties of wind turbine towers.

Study	Material	Variable	Distribution	Mean	COV
[14]	Structural	Young's modulus	Normal	210.0	0.05
[52]	steel	(GPa)	Normal	210.0	0.10
[101]			Lognormal	210.0	0.03
[68]			Lognormal	210.0	0.02
[14]		Yield stress (MPa)	Lognormal	355.0	0.05
[101]			Lognormal	414.0	0.05
[68]			Lognormal	240.0	0.05
[101]		Shear modulus (GPa)	-	80.8	-
[101]		Bending moment (MPa)	Gumbel	165.9	0.02
[14]		Density (kg/m ³)	Normal	8500.0	0.05
		Tower base thickness (m)	Normal	0.027	0.03
		Tower base outside diameter (m)	Normal	6.5	0.03
[52, 132]		Poisson's ratio	-	0.28-0.30	-
[14]		Tower base thickness (m)	Normal	0.03	0.03

generally contained high uncertainties due to difficulties in measurements. In contrast, the water depth was precisely known. Zhao et al. [50] developed a dynamic analysis system of the FOWT employing a beam on a nonlinear Winkler foundation model to investigate the feasibility of soft-soft and soft-stiff design approaches, taking the soil geometric size and stiffness into account that affected the dynamic response in clay.

Soil properties have received the least attention in a probabilistic context among the main factors affecting wind turbines, yet they are vital in determining FOWT systems' response. Although some standards let engineers apply probability-based approaches, the current design practice treats the uncertainty in offshore soil conditions in a deterministic manner. Carswell et al. [138] described how uncertainty in subsea soil's mechanical properties could contribute to significant uncertainty in wind turbines' response to offshore loads. The main sources of soil property uncertainty at potential FOWT locations are the high cost and logistical issues of conducting detailed soil sampling, as well as measuring the in-situ soil properties. Due to the calculation simplifications, the normal (or Gaussian) probability distribution is frequently employed to partially model the variability in soil properties. However, non-Gaussian distributions might also be helpful because numerous soil properties are skewed or are bounded by ranges. Concerning soil properties with lower bounds, Lognormal distributions are commonly employed. DNV also recommends using the beta distribution for soil properties with lower and upper bounds where mean and standard deviation are known. Carswell et al. [138] used a beta distribution model for the soil friction angle property variability (φ) due to the flexibility of the distribution shape which made it possible to analyze different distribution skews in a way that the Lognormal distribution was not capable of. Mardfekri et al. [139] developed a probabilistic model for estimating the moment, shear, and deformation demands of the support structure in OWTs. They used FEA to generate virtual experimental data to calibrate the unknown model parameters. The developed probabilistic model could accurately capture the nonlinear soil-structure interaction, statistical uncertainty, and model errors.

In addition, time-varying waves and currents in an offshore environment make the scour problem more complex than the structures in the river. The scour phenomenon may significantly affect the stiffness, fatigue reliability, and natural frequency of FOWT support structures [140]. Many studies on scouring phenomena in offshore wind farms proposed methods to predict and characterize maximum scour depth and surrounding scour extension. Using the p-y method, the scour phenomenon could be modeled by removing the relevant springs [141]. When using FEA, the scour might be represented by changing the soil's

Table 6Considered material uncertainties of mooring lines.

Study	Material	Variable ^a	Distribution	Mean	COV
[14]	Catenary	Breaking load (MN)	Lognormal	6.65	0.05
[134]		Tension (Line 1) (kN)	Weibull	3000-6000	-
		Tension (Line 2) (kN)	Weibull	3000-6000	-
		Tension (Line 3) (kN)	Weibull	500-1500	-
[135]		Minimum breaking load (kN)	Normal	13000	0.03-0.07
[55]		Minimum breaking load in site 1 (t)	Normal	1394	0.021
[135]	Taut-leg	Minimum breaking load (kN)	Normal	19000	0.03-0.07
[55]		Minimum breaking load in site 2 (t)	Normal	1204	0.023
		Minimum breaking load in site 3 (t)	Normal	1933.1	0.023
	Chain	Minimum breaking load in site 1 (t)	Normal	1423	0.05
		Minimum breaking load in site 2 (t)	Normal	1213	0.05
		Minimum breaking load in site 3 (t)	Normal	2018	0.05
	Polyester	Minimum breaking load in site 1 (t)	Normal	1560	0.05
		Minimum breaking load in site 2 (t)	Normal	1296	0.05
		Minimum breaking load in site 3 (t)	Normal	2052	0.05
[136]	Chain link	Strength of chain link	Lognormal	1.2	0.05
	Steel wire	Strength of steel wire	Lognormal	1.16	0.05
[137]	Catenary	Breaking load capacity (kN)	Lognormal	7334	0.05

^a For the comprehensive definition of the variables, it is referred to the cited literature.

geometrical shape [142]. Breusers et al. [143] described the maximum scour depth subject to steady-state current conditions. Sumer [144] developed a new method for determining the scour depth subjected to only the wave effect. However, this phenomenon has never been defined as a formula or uncertainty of the combined wave and current conditions.

Besides, many offshore sites are made up of sandy silts or loose silty sands, making them prone to liquefaction [145]. In high seismicity regions, soil liquefaction might impose design risks and engineering challenges on the dynamic response of FOWTs due to the strong ground motions. Yet, research considering the impact of seismic liquefaction on FOWTs is very limited. According to ISO 19901-835 4, geotechnical conditions for the anchors must be considered in seismically active regions to assess the potential for liquefaction and dynamic soil properties [146]. Patra et al. [145] investigated the seismic response of a monopile OWT subjected to sand liquefaction under combined seismic and operational loads. They reported that in the case of a small earthquake or seismic event (peak acceleration of 0.1 g–0.2 g), wind and wave loads dominated over seismic load, while in the event of a large earthquake (peak acceleration of 0.3 g–0.4 g), seismic load prevails over wind and

wave loads. This implies the need for a proper combination of wave, wind, and seismic loads for the seismic design of OWTs. Zhang et al. [147] performed dynamic analyses of a 10 MW OWT under earthquake-induced liquefaction subjected to combined wave, wind, and seismic loadings. They reported that the liquefaction was aggravated under the combined wind and seismic loadings, while liquefaction was not significantly affected by the wave loading. Table 7 summarizes the soil conditions and dynamic response uncertainties. Table 7 summarizes the soil conditions and dynamic response uncertainties.

In the context of FOWT design, soil material properties uncertainty, such as soil unit weight, Young's modulus, Poisson's ratio, and cohesion, are commonly represented using the Normal distribution. The uncertainty associated with soil friction angle is often modeled using the Beta distribution, with COV values ranging from 0.05 to 0.20. Furthermore, uncertainties stemming from terrain roughness, landscape topography, lift and drag coefficients, and load-effect computations under external loads contribute to the overall uncertainty, with COV values typically ranging from 0.05 to 0.15, as reported in the literature. To accurately characterize the soil conditions, we emphasize the importance of conducting comprehensive geotechnical investigations, including soil testing and analysis. By incorporating geotechnical uncertainty considerations into the design process, FOWTs can be engineered to withstand diverse environmental conditions and operate reliably throughout their intended service life.

2.4. Growing uncertainties over time

Growing uncertainties over its lifecycle can significantly affect the reliability of FOWT. We identify this as an area of critical research need. The sources of this type of uncertainty can be from the natural change of the material properties due to deterioration or fatigue and from the shift of environmental loads such as winds and waves. This also can be caused by the amendment of the current method of estimation or the restrictions following our improved knowledge.

The current practice to estimate the environmental loads are a simple statistical extrapolation. Although extrapolation techniques are generally well established onshore, this concept provides very limited and unrealistic information in the application of offshore environments due to the large uncertainties involved in offshore environments. Agarwal and Manuel [149] applied a probabilistic approach to predict the extreme wave load. Young et al. [150] investigates global changes in oceanic wave height and wind speed using data from calibrated and verified satellite altimeter collected over a 23-year period. However, growing uncertainty throughout its lifetime has not been investigated nor considered in previous research, while the influence of the growing uncertainties on FOWT reliability is significant.

Fig. 6 presents the effect of the time-variant uncertainties on structural reliabilities. Fig. 6(a) shows the reliability neglecting the time-dependent variance, while Fig. 6(b) exhibits the reliability considering the growing uncertainties over time. The cross-hatching area indicates the reliability of the system where time-variant uncertainty significantly changes its estimation. As shown in Fig. 6, neglecting the uncertainties growing over time might lead to a significant error in the estimation of the life-cycle reliabilities.

As discussed above, failure modes associated with wind turbine structures include several time-dependent phenomena that are important for their design. To investigate the time-varying uncertainties of ocean environmental loads, we suggest analyzing the sets of long-term global wind/wave database: a) Buoy data sets from National Data Buoy Center, NWS, NOAA, b) Model data sets from Environmental Modeling Center, NCEP, NOAA., and c) NCEP CFSRR 30-year homogeneous data set. This section discusses the effect of corrosion, multihazard environment, as well as fatigue damage caused by the ocean environment, resulting in the material's degradation, which ultimately affects its resistance. To assess fatigue loads for FOWTs, it is crucial to comprehensively account for a range of site-specific environmental

Table 7Summary of offshore soil conditions and dynamic response uncertainties

Study	Variables ^a	Soil depth & layer	Distribution	Mean	COV
[44]	Soil effective unit	Layer 1	Normal	16.0	0.05
	weight (kN/m ³)	Layer 2	Normal	17.0	0.05
		Layer 3	Normal	18.0	0.05
	Internal friction	Layer 1	Beta	33.0	0.08
	angle of sand (°)	Layer 2	Beta	35.0	0.07
	ungre or suna ()	Layer 3	Beta	37.0	0.05
[85]	Soil factor	Layer 5	Normal	1.00	0.20
		12 m			
[50]	Young's modulus		Normal	31.5	-
	(MPa)	12.2 m	Normal	20.0	-
		13.3 m	Normal	33.0	-
		14.1 m	Normal	39.0	-
	Poisson's ratio	12 m	Normal	0.35	_
		12.2 m	Normal	0.30	_
		13.3 m	Normal	0.23	-
		14.1 m	Normal	0.25	_
	Cohesion (kPa)	12 m	Normal	4.40	_
		12.2 m	Normal	4.70	_
		13.3 m	Normal	10.8	_
		14.1 m	Normal	5.20	_
	Friction angle (°)	12 m	Normal	33.5	_
	- menon unaic ()	12.11 12.2 m	Normal	33.2	_
			Normal		_
		13.3 m		29.1	
F1 207	Coil friction a 1-	14.1 m	Normal	33.0	- 0.05.0.10
[138]	Soil friction angle		Beta	N/A	0.05-0.10
	property variability		Beta	N/A	0.10-0.15
	(φ)		Beta	N/A	0.15-0.20
[52]	Unit weight (kN/	Sandy	-	10	-
	m3)	soil/loose			
	Unit weight (kN/	Sandy	_	10	_
	m3)	soil/			
		medium			
	Unit weight (kN/	Sandy	_	10	_
	m3)	soil/dense			
	Young's modulus	Sandy	_	30	_
		•	_	30	_
	(MPa)	soil/loose		50	
	Young's modulus	Sandy	-	30	_
	(MPa)	soil/			
	371	medium		00	
	Young's modulus	Sandy	-	80	-
	(MPa)	soil/dense			
	Angle of friction (°)	Sandy	-	33	-
		soil/loose			
	Angle of friction (°)	Sandy	-	35	-
		soil/			
		medium			
	Angle of friction (°)	Sandy	_	38.5	_
		soil/dense		00.0	
	Cohesian (LDa)			50	
	Cohesion (kPa)	Sandy	-	30	_
	Onlandar (LD.)	soil/loose		F0	
	Cohesion (kPa)	Sandy	-	50	-
		soil/			
		medium			
	Cohesion (kPa)	Sandy	_	50	-
		soil/dense			
	Yield stress (kPa)	Sandy	_	59.2	_
	,,	soil/loose		- · · -	
	Yield stress (kPa)	Sandy	_	58.5	_
		soil/			
		medium			
	Yield stress (kPa)	Sandy		57.0	
	riciu sucos (Kra)	•	_	37.0	_
	Emission Confficient	soil/dense		0.40	
	Friction Coefficient	Sandy	-	0.40	-
		soil/loose			
	Friction Coefficient	Sandy	-	0.43	-
		soil/			
		medium			
	Friction Coefficient	Sandy	_	0.48	_
		soil/dense			
F1.4Q1	Effective unit weight	_	_	_	0.1
[140]	Friction angle	_	_		(), 1
[140]	Friction angle	_	_	_	0.1
[148]	Coefficient of lateral	-	_	_	0.1
[140]	-	_	-	-	

(continued on next page)

Table 7 (continued)

Study	Variables ^a	Soil depth & layer	Distribution	Mean	COV
	Shear modulus of elasticity	-	-	-	\times or \div 5
	Initial modulus of subgrade reaction	-	-	-	\times or \div 2
	Position of characteristic soil layer transition	_	-	-	±1 m

^a For the comprehensive definition of the variables, it is referred to the cited literature.

conditions throughout the system's expected lifespan. This includes wind direction, wind speed, turbulence intensity, wind shear, wave direction, wave height, wave period, wind-wave misalignment, yawed inflow, current direction, current speed, as well as factors like ice and marine growth [152]. Compared to fixed-type offshore wind turbines, FOWTs are more sensitive to variations in environmental conditions, necessitating the consideration of a larger number of conditions with higher resolution. Specifically, the importance of wave period and directionality becomes more significant in fatigue load analysis for FOWTs.

Hübler et al. [153] conducted an assessment of long-term environmental conditions for fixed-type OWTs by employing various models to predict changes in wind speed and air temperature, while considering associated uncertainties. These predictions were then used to forecast the environmental conditions experienced by FINO3 which is a meteorological tower (meteorological mast or met mast) throughout its lifespan. The study highlighted that the expected changes in fatigue damages over the tower's lifetime were relatively small compared to other sources of uncertainty in fatigue damage calculations. Furthermore, the analysis indicated shifts in the air density and wind speed distributions, resulting in an increased likelihood of extreme wind speeds. Consequently, slightly higher wave heights were observed compared to scenarios with constant wind speeds. It was observed that fatigue loads would experience a slight increase (below 5%) due to the anticipated effects of rising wind speeds and air temperatures over the next 25 years. They reported that considering the larger uncertainties in lifetime calculations, the inclusion of climate change effects in current lifetime calculations for OWTs or FOWTs is deemed unnecessary. Nonetheless, this may change if lifetime calculations become more accurate or if climate change intensifies.

Grabemann et al. [154] used the WAM wave model and analyzed a 30-year period from 2071 to 2100 to investigate the potential future changes in mean and extreme wave conditions in the North Sea due to anthropogenic climate change. They employed an ensemble of wind field data sets from four climate change scenarios driven by two global circulation models. The results showed that the long-term 99th percentile wind speed and significant wave height in the North Sea could

increase by up to 7% and 18% respectively. Variations in climate change patterns were observed among the scenarios and model combinations, with higher uncertainties in the northern part of the North Sea. The findings indicated a moderate rise in extreme wind speeds and wave conditions in the eastern region of the North Sea by the end of the 21st century, emphasizing the need for appropriate planning and adaptation measures for coastal and offshore activities. The study also revealed that extreme wave heights could potentially increase by around 0.25 m-0.35 m (5-8% of present values) in the southern and eastern North Sea under global warming conditions. The northern part of the North Sea exhibited the highest uncertainties in the climate change signals, with uncertainty ranges of up to 0.6 m-0.7 m for extreme wave heights south of the Norwegian coast and up to 0.9 m/s for extreme wind speeds off the Danish coast. Conversely, the southwestern part of the model domain, towards the English Channel, showed the smallest model-related uncertainties of approximately 0.1 m for extreme wave height and 0.2 m/s to 0.4 m/s for extreme wind speed.

Recent research using global wind data from in-situ stations has revealed that the global decline in average surface wind speed, known as global terrestrial stilling, has reversed since around 2010 [155]. This recovery in wind speeds is attributed to internal decadal ocean-atmosphere oscillations, suggesting a continued rise for the next decade with potential future declines. This positive trend supports the expansion of wind power as a renewable energy source, offering environmental benefits and opportunities for large-scale and efficient wind power generation systems, particularly in mid-latitude countries. The analysis also indicated a $17\pm2\%$ increase in potential wind energy and a 2.5% boost in the wind power capacity factor in the United States.

2.4.1. Corrosion and deterioration

The main disadvantages of FOWTs are the difficulty of access and harsher environmental conditions such as higher humidity leading to corrosion and oxidation. This significantly increases operation and maintenance costs. To optimize the maintenance costs, extensive experimental data is needed to assess the reliability of structures using probabilistic approaches. Also, defining the proper distribution types as well as quantifying the mean and standard deviation values is vital to achieving accurate reliability analysis [5]. To this end, obtaining data from condition monitoring (CM) and structural health monitoring (SHM) could be used to provide valuable information concerning the condition of FOWTs over a long project's service life.

Steel chains in mooring lines that are in contact with seawater undergo corrosion, degrading their physical and mechanical properties due to section loss. Reduction in the material thickness due to corrosion could also make it vulnerable to buckling and fatigue crack nucleation and propagation, leading to the structure's failure [52]. The severity of this section loss depends on the water type, part of the mooring line involved (e.g., bottom, catenary, and splash zone), and inspection type [9]. Dong et al. [156] studied the impact of a salt fog environment on the

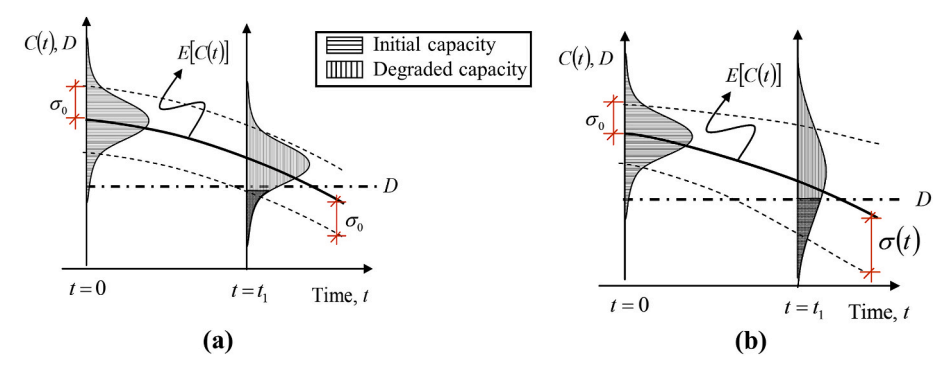


Fig. 6. Effects of the time-variant uncertainty on structural reliability: (a) considering a constant variance, and (b) considering a time-dependent variance. (E[C(t)]: mean capacity, D: given demand, σ_0 : initial standard deviation, and $\sigma(t)$: standard deviation at the time t) [151].

structural damage of offshore wind turbine blades. The pitted blade surface formed by the milling and pumping of sand blown by the wind was found to be the incentive. Also, ultraviolet radiation and water molecule diffusion were found to be the main reasons for blade degradation.

2.4.2. Multi-hazard environment

FOWTs are characterized as towering structures, meaning a slight pitch motion of the support platform might result in large displacements of the turbine rotor. Thus, it is vital to evaluate their dynamic response subjected to extreme sea states. Extreme wind conditions are defined with regard to air density in conjunction with wind events. The peak wind speeds and wind shear events caused by storms, extremely rapid changes in wind direction and speed (wind gusts), and extreme turbulence are examples of extreme wind conditions [157]. Wind direction and speed fluctuate at different scales in space and time. For wind loads simulation, the period of particular interest ranges from several days to a few seconds [158]. There high-frequency oscillations (i.e., small-scale and short-term fluctuations in wind speed) and low-frequency oscillations (long-term wind statistics) exhibit a spectral gap that shows the low energy content in these ranges. Subsequently, when a stationary stochastic process is assumed, the error is minimized, and the wind can be represented separately for the lower-frequency and the higher-frequency ranges [158]. FOWTs are subjected to climate change hazards such as hurricanes (central and eastern North Pacific Ocean), and typhoons (northwest Pacific Ocean; usually east Asia). Failures of OWTs due to typhoons are regularly reported. For example, typhoon Usagi struck the Honghaiwan wind farm located in Coastal Shanwei City in China and knocked out 17 out of 25 offshore wind turbines, resulting in a loss of \$16 million to the wind farm [159]. In addition, FOWTs are exposed to potential earthquake hazards. Seismic events influence the FOWT structures differently based on the station-keeping arrangements. In the case of catenary lines, earthquake motions may lead to dynamic mooring line tension loading which is a critical factor for the station-keeping system, while its effect on the turbine and floater is minimal. Concerning taut systems, however, the seismic motion might be transferred directly to the floater [146]. Therefore, developing advanced reliability models considering these environmental and climate change hazards is vital.

2.4.3. Fatigue

FOWTs undergo significant environmental cyclic loads. Therefore, their design is generally dominated by fatigue limit state [160]. For structural integrity over a long period of operation, the fatigue effects of these coupled loads can be critical to the design of floating wind platforms. Areas of fatigue concern include the turbine tower to hull connection, the connection of the mooring to the floating foundation, and possibly the anchor connection. This can also be at any primary structural connections such as between any columns and pontoons, columns, and deck connections, or between upper and lower girder connections depending on the foundation design. Welding connections are particularly known to be vulnerable connections under fatigue. The methods for fatigue analysis to assess fatigue reliability could be categorized into two main classes S-N curve and fracture mechanics methods [161,162]. The crack growth data of an initial flaw is necessary for the fracture mechanics approach, while the S-N curve method which assumes constant amplitude stress cycles requires the S-N fatigue test data to generate S-N curves using statistical analyses such as maximum likelihood and least square methods [5]. The parameters associated with the fracture mechanics and S-N methods are dependent on the environmental condition, material types, and the utilization of corrosion protection.

Fatigue loads, in current engineering practices, are generally evaluated through extensive time-domain simulations of different load cases. Because of a variety of environmental loads (e.g., wave direction, wave height, current, and wind) a full fatigue limit state (FLS) analysis might

become computationally expensive. Therefore, efforts have been made to propose simplified methods for quick frequency domain load analysis [85,163,164].

In addition, FOWTs face potential failure cases and accidents including ship collisions, ice-related issues, and fire incidents [165]. To mitigate these risks, robust collision avoidance systems, anti-icing measures, and fire detection and suppression systems are essential. Comprehensive risk assessment, proactive maintenance, and continuous monitoring are crucial for ensuring the safety and reliability of FOWTs. The industry is continuously learning and evolving regulations and standards to enhance the resilience and integrity of these structures.

2.5. Modeling uncertainties

Another important type of uncertainty is modeling uncertainty which is typically associated with our lack of describability of the system or the modeling assumption for the sake of simplicity. The modeling uncertainties can be addressed by a simple addition of a certain model standard deviation. The most common type of distributions for the modeling uncertainties are either Normal or Lognormal distribution [20, 166], although Lognormal distribution is more commonly used due to the mathematical limitation which bounds above zero (0). Modeling uncertainties in their study included modeling of exposure, assessment of lift and drag coefficient, and the computation of load-effects under external loads. Modeling uncertainties that have been applied to the model and statistical parameters of FOWTs are presented in Table 8.

3. Reliability analyses

3.1. Available reliability methods

Limit state function (LSF) represents the failure status for various failure modes of the systems. The LSF is formulated such that the negative value of LSF represents the failure. In structural reliability, it is generally expressed concerning stress, strain, displacement, and modal frequency [5].

Structural reliability can be expressed in terms of either the probability of failure or the reliability index. The probability of failure represents the probability of the LSF at the negative value. The analyses can be performed at various levels: from the conditional probability of failure given the extreme events at the components lever, i.e., for specific element designs (univariate), to the probability of system failure considering the failure scenarios over the lifetime (multivariate and time-variant). These probabilities of failures, P_f , can also be converted in the form of the reliability index, β , with a simple expression as follows $\beta = -\Phi^{-1}(P_f)$, where Φ indicates the normal distribution function [171-173]. As expressed, a higher reliability index indicates a lower probability of failure. In addition, the exponential function within Φ enables the reliability index to emphasize the reliabilities within the range of our interest, i.e., the probabilities of the failure close to 0. For instance, the probability of failures of 1.0E-4 and 1.0E-5 can be converted into the reliability index of 3.72 and 4.26 respectively, which increased scale allows us to emphasize the different levels of risks. DNV 2016 [174], specify the target reliability index of FOWT support structures is usually considered 3.72 equivalent to a failure probability of 0.0001.

To estimate the probability of failure, the failures are first defined in the form of the LSF, $g_k(X,\theta)$, for each potential failure mode k, where X represents the vector of the random variables discussed in this paper and θ represents a vector of statistical variables that can be obtained from the observations to improve our knowledge. LSF is expressed as $g_k(X,\theta) = C_k(X,\theta) - D_k(X,\theta)$ where $C_k(X,\theta)$ represents the capacity model, such as a strength or drift, and $D_k(X,\theta)$ represents the demand model, such as the required strength from the environmental loads. The models can be defined for the structural component level corresponding to the failure

Table 8Modeling uncertainties used in FOWT.

Study	Variable ^a	Distribution	Mean	COV
[14]	Yield model uncertainty	Lognormal	1	0.05
	Exposure (terrain)	Lognormal	1	0.1
	Structural dynamics	Lognormal	1	0.05
	Aerodynamic parameters	Lognormal	1	0.1
	Hydrodynamic parameters	Lognormal	1	0.1
	Load effect computation	Normal	1	0.03
[167,	Loading for mooring lines	Lognormal	1	0.17
168]	Material properties for mooring lines	Lognormal	1	0.03
[20]	Mean wind speed	Gumbel	1	0.23
	Load carrying capacity	Lognormal	1	0.05
	Limited wind data	Lognormal	1	0.10
	Dynamic response	Lognormal	1	0.05
	Exposure	Lognormal	1	0.20
	Lift and drag coefficients	Gumbel	1	0.10
	Stress calculation	Lognormal	1	0.03
[68]	Exposure (terrain)	Lognormal	1	0.2
	Climate statistics	Lognormal	1	0.1
	Structural dynamics	Lognormal	1	0.1
	Shape factor/model scale	Gumbel	1	0.1
	Stress evaluation	Lognormal	1	0.03
	Scale effect for yield stress	Lognormal	1	0.05
	Scale effect for Young's modulus	Lognormal	1	0.02
	Critical load capacity	Lognormal	1	0.1
[169]	Dynamic response including	Lognormal	1.00	0.05
	uncertainty in eigenfrequencies and			
	damping ratios, X _{dyn}			
	Terrain roughness and landscape	Lognormal	1.00	0.15
	topography, X _{exp}			
	Lift and drag coefficients, Xaero	Gumbel	1.00	0.10
	Computation of the load-effects given	Lognormal	1.00	0.03
	external load, X _{str}			
[170]	Linear damage accumulation	Lognormal	1	0.30
	Blade Elements	Weibull	1	0.05
	Uncertainty in full-scale tests	Weibull	1	0.05
	Structural dynamics	Lognormal	1	0.05
	Exposure	Lognormal	1	0.2
	Climate statistics	Lognormal	1	0.1
	Shape factors	Gumbel	1	0.1
	Stress evaluation	Lognormal	1	0.03
	Simulation statistics	Normal	1	0.05
	Rainflow counting	Lognormal	1	0.02

^a For the comprehensive definition of the variables, it is referred to the cited literature.

mode k. The probability of failure for k-th failure mode is defined as $P_f = P(g_k(X, \theta) < 0) = P(C_k(X, \theta) < D_k(X, \theta))$ [175]. The probability of system failure is defined as the logical union of the probabilities of failures corresponding to each failure mode, expressed as $P\left[\bigcup \{g_k(X, \theta) < 0\} \middle| X, \theta\}\right]$

 θ . General form of the time-variant structural capacity $C_k(t,X(t),\theta)$ and demand models $D_k(t,X(t),\theta)$ are introduced by Choe et al. [176,177] for the first time to estimate the time-variant structural reliability with an example of corrosion of steel elements within concrete structures. The growing uncertainties, $\theta(t)$, for the structural components are introduced and discussed with an example of the fragility of concrete bridge column problems [151]. DNV 2016 [174] presents four types of LSF: 1) ultimate limit state (ULS) to resist plastic collapse, 2) fatigue limit state (FLS) to resist cyclic loads, 3) serviceability limit state (SLS) to resist excessive deflection, vibration, and buckling, and 4) accidental limit state (ALS) to resist infrequent loads such as earthquake and explosion. The main failure modes of FOWTs could be classified as plastic collapse, fatigue, excessive deflections, vibration, and buckling [5].

Generally, typical methods of structural reliability estimation can be categorized into two main groups 1) sampling (or simulation) methods and 2) approximation methods. A general idea of the sampling method such as Monte Carlo simulation (MCS) is to generate an acceptable number of the most probable samples to observe the actual uncertainties of the system. MCS is the foundation for sampling methods where the

failure probability could be evaluated via both explicit and implicit performance functions. MCS performs repetitive simulation processes via random sampling of input variables to calculate the accurate probability of failures [178]. Nevertheless, MCS is computationally expensive especially when dealing with complex problems with implicit performance functions and/or low failure probabilities. To improve the efficiency, other sampling methods such as importance sampling [179], adaptive sampling, Latin hypercube sampling [180], subset simulation [181], and directional simulation [182] have been proposed. Markov Chain Monte Carlo (MCMC) [183] is one of the widely-used sampling methods and was proposed for sample methods that enable us to approximate the statistical properties of the system.

The approximation methods, on the other hand, use a local approximation of the limit state function to evaluate the probability of failure through various methods such as the First-Order Reliability Method (FORM), Second-Order Reliability Method (SORM), First-Order Second Moment (MVFOSM or FOSM), Response Surface Method (RSM), etc. The MVFOSM method estimates the mean and variance of the response to calculate the reliability index (β) via the first-order Taylor series approximation of the response and its derivatives at the random input variables' mean values [184]. The MVFOSM method leads to inaccurate estimations when the performance function is nonlinear, and the input random variables do not follow Normal distribution (i.e., they are non-Gaussian). To overcome these limitations, design point-based methods (FORM and SORM) can be utilized to assess the limit state function at the design point (also called the most probable point (MPP) or β -point) in the standard normal space. FORM uses the first-order Taylor expansion (linear) of the limit state function in the standard normal space, while SORM employs the second-order Taylor expansion (parabolic) to estimate the limit state space at the design point [185].

Generally, the approximation methods predict the probability of failure quite accurately. However, if the limit state is multimodal (multiple MPPs) or its surface is greatly non-flat, they may fail in solving the problem. Although RSM could work, it might not provide accurate approximations. In such cases, global reliability methods such as AK-MCS (Active learning reliability method combining Kriging and Monte Carlo simulation) and EGRA (efficient global reliability analysis) can be used [186,187]. Global reliability methods estimate the performance function using a Gaussian process (or Kriging model) which can model the nonlinear limit state function sufficiently, and then employ sampling methods to estimate the probability of failure using surrogate models that significantly reduce the computational cost.

3.2. Review of existing uncertainty analyses

There are several efforts made for the uncertainty modeling for the structural reliability of fixed-type offshore wind turbines considering limited uncertainties on wind turbine structures or environmental loads [139,149,188,189]. However, very few studies are available on structural reliability that accounts for the uncertainties that existed in floating structures, mooring lines, and hydrodynamics. This section describes uncertainty models related to offshore wind turbines' structural components and systems. Furthermore, reliability analyses concerning growing uncertainties over time are presented.

3.2.1. Turbine blades

The methods for improving the reliability of giant wind turbine blades have been investigated by many researchers. Nevertheless, the floating offshore wind turbine's risk assessment is yet insufficient due to the lack of experimental data. When their foundation is subjected to 6-DOF motions under wind, wave, and current loadings, the blade's unsteadiness worsens and the blades exhibit higher peak loads and fatigue damage compared to the onshore and fixed-type OWTs [190].

Liu et al. [129] conducted a reliability analysis for the blades of the FOWTs. The structure failures of the blade could be attributed to three scenarios: 1) fatigue damage, 2) serious damage and breakage accidents,

and 3) general deficiencies. It was assumed that the fatigue limit state followed a normal distribution, while the blade root stress followed the Lognormal distribution. The displacement amplitude of a blade tip was dealt with as normal distribution. The blade tip flap-wise motion's amplitude almost followed a normal distribution. It was concluded that the probability of failure of blades supported by floating foundations was higher than that of a fixed-type foundation.

Gonzaga et al. [122] used Monte Carlo simulation to characterize and propagate uncertainties in a blade structural model.

3.2.2. Floating structures

The sources of uncertainties inherent to the floating structures include potential high power output fluctuation towing to motions, potential instability by blade pitch control, and increased inertia loading from motions [191]. Due to the observation of significant dynamic effects in floating structures, the simulation of wave elevation and environmental loads requires consideration of randomness and uncertainties [83]. To predict the long-term design loads of OWTs with minimum computational effort, Karmakar et al. [72] took advantage of the environmental contour method. The floating structure's shape is one of the main aspects affecting the shape parameter in Weibull distribution describing wave-induced loadings [192]. Zhao and Dong [193] performed a structural reliability analysis of floating platforms using response-based and environmental contour methods. The floater offset was found to be one of the most significant criteria for the reliability assessment of the floating structure. The existence of system failure modes with non-structural nature and strong interaction between structural and non-structural component failures are considered as main obstacles to the proper application of structural reliability methods on floating structures [194].

3.2.3. Mooring lines

Based on an R3 chain grade of DNVGL–OS–E301 [195], assuming the breaking load of the mooring line as a Lognormal distribution, the reliability of the FOWT placed at a water depth of 320 m was evaluated [14], and robust reliability analysis of FOWT was presented. Hsu et al. [134] proposed a composite Weibull probability distribution for the dynamic tension of the mooring line that took snap events into account. When snap events are not taken into account, the maximum tension on FOWT mooring systems might be underestimated. It was found that models simulated using Weibull distribution underestimated the upper tail of the dynamic tension which includes snap events. When the probability of shock load incidence is greater, the developed composite Weibull distribution model may provide a good starting point for predicting extreme dynamic tensions of the mooring system. Generally, for rare events with high peak responses, the Gumbel distribution outperforms in extracting extreme responses.

Horte et al. [136] performed structural reliability analysis in order to calibrate a design equation for FOWT mooring lines in their ultimate limit state. The calibration was done based on six test scenarios for mooring systems in water depths ranging from 70 m to 2000 m. Several studies have been done on traditional catenary mooring systems that include wire and/or chain components. It was assumed that the strength of chain link and steel wire mooring lines were distributed using a Lognormal function. It should be noted that in current engineering practices, conventional catenary mooring system is not used in deep water (>500 m) where the chain-wire-chain system (semi-taut mooring) and chain-polyester-chain (taut mooring) system are considered more efficient solutions. Hou et al. [196] also assumed a Lognormal distribution function to model the allowable strength of mooring lines. Liu et al. [197] performed a reliability analysis of mooring lines of FOWTs using Teaching Learning Based Optimization (TLBO) algorithm. The variables included in the limit state function of mooring systems were defined to be axial tension and breaking strength, where both followed a normal distribution. The average breaking tensile strength of three mooring lines was 13,583 kN with a standard deviation of around

2717.0 kN.

Zhao et al. [198] proposed a method based on a Bayesian network inference-artificial neural network to evaluate the reliability of mooring lines subjected to extreme environmental conditions. Since Bayesian inference requires a large database in order to estimate a reasonable posterior probability, the artificial neural network was used for numerical data simulations to improve computational efficiency. Then, the failure probability of mooring lines in a semi-submersible floating platform was evaluated based on the allowable breaking strength as a limit state function. The failure model of the mooring system was simulated using the Bernoulli distribution. The probability of failure exhibited a significant increase at higher extreme wave heights. In another study, Rendon et al. [135] investigated the reliability index and predictive reliability of mooring lines subjected to extreme metocean conditions taking into account the impacts of parameter uncertainty. A first-order analytical formulation was developed to account for the uncertainty in parameters for maximum breaking and dynamic tension resistance of mooring lines. The breaking resistance of mooring lines was assumed to have a known mean value and its standard deviation was uncertain. Also, the maximum dynamic tension of mooring lines was modeled as a stationary Gaussian process since the random variables were functions of the peak spectral period and the significant wave height. The predictive reliability and probability of failure were insensitive to parameter uncertainty in probability distribution of mooring lines breaking resistance, while they were quite sensitive to the statistical uncertainty in the probability distribution of dynamic tension loading. In addition, considerable discrepancies were observed between the mean and predictive reliability indices.

Montes et al. [55] formulated a nested reliability analysis of the mooring line's ultimate limit state (ULS) considering the uncertainty in the mooring line's maximum dynamic tensions, which was evaluated conditionally on the uncertain environmental variables. Response surfaces were employed to express the distribution parameters of the maximum dynamic tension as well as the mean mooring line tension as functions of the environmental parameters. Because sea waves are considered a Gaussian process, and the mooring lines' dynamic tension is mainly governed by the first-order response, the dynamic tension was considered to be approximately Gaussian. Then, the developed nested reliability formulation was used to calibrate the partial safety factors for ULS with a target reliability index of 4.4. It was found that assuming significant wave height and peak period as random variables and current velocity and wind speed as deterministic variables resulted in similar safety factors with only a 2% overestimation in reliability indices compared with the full model.

3.2.4. Corrosion and deterioration

Andrawus and Mackay [199] developed a predictive maintenance strategy based on a risk assessment method for corrosion resistance and protective coating of offshore wind turbine blades. The risk was determined as the product of the likelihood of occurrence (characterized by the coating history factor) and the failure consequences of the turbine blade (represented by the sum of the total cost of material, labor, access, and production losses). Dong et al. [200] conducted a reliability analysis of OWTs considering the effects of corrosion and inspection. They used a 2-p Weibull distribution to fit the statistical distribution of hot-spot stress ranges subjected to combined wind and sea states environmental conditions. The fracture mechanics of crack growth caused by corrosion were used in the reliability analysis. The main sources of uncertainty were identified and quantified based on the inspection quality in terms of the crack detection probability curves. In addition, corrosion-induced geometry and material degradation effects on the reliability analysis were investigated, and the reliability index sensitivity on stochastic variables was evaluated. Shittu et al. [201] also assessed the reliability of OWT support structures under pitting corrosion-fatigue using probabilistic models. The first order reliability method (FORM) was employed to estimate the reliability index of components. It was found that the structure became unsafe at the age of 18 years, before reaching a typical service life of OWTs. Also, the results revealed that the pits' aspect ratio at critical size had a substantial impact on the structural reliability.

3.2.5. Multi-hazard environment

Tarp-Johansen et al. [202] studied the structural reliability of offshore wind turbines in the Philippines exposed to severe typhoon hazards. They derived the safety factors to be applied to characteristic loads based on 50-year extreme 10-min mean wind speeds. They reported that to achieve a similar reliability index using FORM analysis, different design wind load specifications should be considered for regions with and without typhoon hazards. This is due to the fact that the reliability of turbine structures under extreme wind loads is affected by the wind coefficient of variation. Although there was some uncertainty regarding the assumptions used to determine the proper distribution of extreme wind speeds due to typhoons, a partial safety factor of 1.7 exhibited the best estimate. Rose et al. [203] developed a probabilistic framework to predict the number of OWTs in a wind farm that could be damaged when subjected to hurricanes in four locations in the Gulf coast and Atlantic waters of the United States. The order of the riskiest locations to install OWTs was as follows: 1) Galveston County, TX, 2) Dare County, NC, 3) Atlantic County, NJ, and 4) Dukes County, MA. The results indicated that almost half of the OWTs would be destroyed during the wind farm's 20-year service life at the riskiest location. More specifically, the Monte Carlo simulation revealed that up to 6% of the turbine towers would buckle subjected to a category 2 (wind speed ≥ 45.0 m/s) hurricane, while a category 3 (wind speed ≥ 50.0 m/s) hurricane could buckle 46% of the turbine towers. The tower buckling was a function of the frequency of hurricane occurrence and its intensity. More turbine towers would buckle at higher intensity hurricanes, yet they occur less frequently.

Mardfekri and Gardoni [204] proposed a probabilistic model to investigate the structural damage of 5 MW OWTs under extreme wind and seismic hazards. Virtual experimental data was generated using FEA to develop the probabilistic models using a Bayesian approach for estimating moment and shear demands and fragility of support structures. They assessed the annual failure probabilities for two identical OWTs at two different locations: 1) California Coast prone to high seismic region, and 2) Gulf of Mexico of the Texas Coast subjected to hurricanes. A higher risk of failure was found for OWTs installed on the California Coast due to high seismicity. Katsanos et al. [205] examined the structural performance of OWTs under a multi-hazard environment (earthquake excitations, wind, and wave loads) using nonlinear time-domain analysis. They employed advanced aero-servo-elastic code to model various parts of the turbine. They reported that wind turbine reliability and tower dynamic response were significantly influenced by the earthquake excitations. More specifically, fragility analysis revealed that even at low-to-moderate seismic excitations, the highly tuned and sensitive equipment that is commonly located at the nacelle was prone to significant damage. Further studies are necessary to develop reliable models considering the environmental and climate change hazards of FOWTs.

3.2.6. Fatigue

Velarde et al. [206] conducted a fatigue reliability analysis for a large monopile 10 MW OWT. The results indicated that potential resonant responses and wave-induced fatigue load could have substantial effects on the fatigue damage which was evaluated by Miner's rules using the S-N curve method. They recommended a reliability-based calibration of fatigue design factor of greater than or equal to three using the FORM. In addition, the sensitivity of the fatigue reliability was quantified against various stochastic input variables. Vahdatirad et al. [207] proposed a probabilistic-based Monte Carlo simulation and finite element model to perform reliability analyses of gravity-based OWTs regarding their bearing capacity. The results were then used to fine-tune

a deterministic-based design code, leading to a 20% saving in materials for the concrete foundation at a similar annual target reliability level. Morato and Sriramula [208] performed structural reliability analysis of OWTs using a Kriging surrogate model to estimate the load-effect using aero-elastic simulations. Thereafter, they calibrated available partial safety factors (PSFs) using probabilistic models. The results indicated that a PSF of 1.31 was required for the target reliability index of 3.09, confirming that PSFs from the IEC 61400-3 were adequate. Also, very low failure probabilities were achieved for most sever design cases. Horn and Leira [45] carried out a fatigue reliability assessment for a monopile OWT with its availability modeled as a random variable which reduced the failure probability and increased its operational lifetime. Environmental parameters such as wind, wind sea, tide, and swell with corresponding directional statistics were considered. They used normal and 3-p Weibull distributions truncated at $\pm 90^{\circ}$ to model the wave heights and relative wind-wave direction, respectively. The results exhibited around a 10% increase in the operational lifetime in the case of employing a beta-distributed availability model of 94% with a standard deviation of 4 instead of using a deterministic availability of 90%. In another study, Horn and Jenson [71] improved the accuracy of fatigue estimations using combined FORM and Monte Carlo simulations (MCS). Dong et al. [200] used fracture mechanics method to predict the fatigue reliability of a fixed jacket OWT taking into account the impacts of corrosion and inspection. They used a 2-p Weibull to fit the long-term statistical distribution of stress at hot-spots. The results indicated a decrease in the reliability index in the case of corrosion and material degradation. The reliability index exhibited a considerable sensitivity to detectable cracks than initial crack sizes. The reliability index of 0.4-0.5 could be achieved if applied the proper inspection and repair strategy.

To date, very limited research has been performed on the fatigue reliability assessment of FOWTs. Li and Zhang [209] developed a probabilistic accumulated long-term assessment of fatigue integrating canonical vine (C-vine) copula and surrogate models on a FOWT (spar-type) under realistic environmental conditions. Two surrogate models (artificial neural network and Kriging model) were used to $model \ the \ nonlinear \ load \ mapping \ relationship \ for \ predicting \ short-term$ fatigue damage in critical areas. Then, sensitivity analyses were performed to study the relative significance of six wave and wind-related environmental loads on the short-term fatigue damages at three critical locations of mooring lines: 1) fairlead, 2) tower base, and 3) tower top. The results indicated that short-term fatigue damage was remarkably sensitive to variations in the mean wind speed and direction. Thereafter, short-term fatigue damage uncertainties were incorporated into a probabilistic fatigue model using the Monte Carlo simulations to predict long-term fatigue damages. It was found that mooring lines that were arranged in the direction of the dominant wave were prone to fatigue damage. Also, locations along the direction of the dominant wave at the base and top of the turbine tower were most vulnerable to long-term fatigue damage. In addition, the influence of wind on long-term fatigue damages was more significant at the tower top than at the tower base. In another study, Li and Zhang [59] predicted the long-term design loads for a FOWT (spar-type). The multivariate dependence structure of six wave and wind-related environmental parameters that affected the dynamic responses was assessed using the C-vine copula model that was integrated into the environmental contour methodology. To evaluate the long-term (50-year) design loads and taking into account the response uncertainty, extreme value distributions for extreme short-term responses were obtained using several dynamic simulations. The results indicated that 300 environmental conditions were sufficient for accurate predictions. Also, it was found that the response uncertainty significantly affected the long-term design loads.

Ziegler et al. [85] developed a computational model to efficiently evaluate the fatigue damage subjected to wave loads using frequency-domain analysis. This model provided better insights into the sensitivity of fatigue loads to various environmental parameters such as

significant wave height, mean sea level, and wave peak period. The frequency-domain analysis, however, is not widely accepted by classification societies (such as the American Bureau of Shipping (ABS), Det Norske Veritas (DNV), etc.). Chen and Basu [114] studied the impacts of current load and its interaction with wave load on the fatigue of a FOWT having a spar-type platform. They concluded that the current had a significant impact on the turbine tower responses and the mooring lines' mean tensions due to the static offset. When ignoring the wave-current interaction, the fatigue life of mooring lines was overestimated. Li et al. [51] investigated the short-term fatigue damages of a 5 MW FOWT (spar-type) at the tower base. Realistic environmental conditions were taken into account to evaluate the structural stresses and loads at the base of the turbine tower. They concluded that fatigue damages induced by the wave were larger than those induced by the wind loads. In the case of a fatigue load, it was confirmed that it exhibited more sensitivity to the counting method of cyclic loads, but not to the simulation length

The correlation between strength and stiffness degradation was studied by Gao and Yuan [210] who presented a probability model representing FRP material's stiffness degradation of a turbine blade. According to their research, the FRP stiffness degradation exhibited a substantial influence on its reliability and fatigue life. Generally, the full-scale level and the element level (which includes local defects and size effects) exhibit similar model and statistical uncertainties.

To consider the model and statistical uncertainties, Weibull distribution was employed by Toft and Sørensen [170] to model both full-scale (X_{full}) and element-scale (X_{elem}) uncertainties. The accumulated damage is usually modeled using a Lognormal distribution to prevent negative values of Miner's rule [20]. A Weibull distribution can adequately approximate the long-term distribution of wave-induced loading. A Weibull distribution on material strength in fatigue may describe the time to crack initiation [211]. An exponential distribution exhibits sufficient approximation for the long-term distribution of wave-induced loads. An exponential distribution can also describe the likelihood of crack detection [192]. Fatigue lives of materials are generally modeled by 2-p Weibull distribution [193].

Müller et al. [152] employed Monte Carlo-based sampling procedures based on Sobol' sequences to address the large variation in environmental conditions for FOWTs. This approach allowed for efficient coverage of the design space and faster convergence with fewer simulations. The analysis focused on the DTU 10 MW reference turbine, using statistical properties of wind speed, wave height, and wave period from Gulf of Maine (USA) measurements. The study demonstrated that approximately 200 simulations were adequate to achieve less than 10% uncertainty in lifetime fatigue damage-equivalent loading. These findings provide valuable insights into quantifying uncertainties based on the number of simulations, facilitating the definition of safety factors. Designers can now choose between a fast approach with fewer simulations and larger safety factors or a detailed approach with more simulations and smaller safety factors.

4. Conclusions and Future Prospects

It is expected that wind power will soon become one of the primary electricity generators, with colossal floating offshore wind turbines (FOWTs) outperforming the industry. Nevertheless, FOWTs are subjected to large structural vibrations due to the coupled effects of aerodynamic and hydrodynamic loads, leading to more frequent failures than fixed-type offshore wind turbines. Therefore, a reliable design of FOWTs considering various sources of uncertainty is the key to structural integrity and serviceability, as well as reducing the cost of energy. Traditional design approaches that consider partial safety factors and load factors to deterministically accommodate these uncertainties using discrete values may lead to either over-designed or under-designed practices. Recognizing this issue, the current review first identifies and presents various sources of uncertainty that might be related to

stochastic variables including uncertainties in environmental loads (e.g., the randomness of the wave and wind loads), material properties of the structural components, as well as growing uncertainties over time such as corrosion and fatigue effects. Then, appropriate statistical distributions for each investigated stochastic variable are discussed to improve the reliability of FOWT systems. These input uncertainties could then be incorporated within probabilistic models to predict the uncertain outputs of the correlations between the stochastic variables as well as model error. The probabilistic design approach might be further studied to establish a basis for the quantification of uncertainty in ultimate design conditions through reliability analysis, providing insight into FOWTs' performance as well as their maintenance requirement. The following conclusions are made.

- Uncertainties in environmental loads: the structural design of FOWTs must account for aerodynamic and hydrodynamic systems. The coupling of uncertainties between them, in addition to the coupling of the dynamic systems, is a critical component in the estimation of the structural reliability of the FOWT system. To do so, an accurate prediction of each uncertainty model, such as stochastic wave, current, and wind loads, is crucial to building confidence in the design process. These uncertainty models should reflect both the uncertainties inherent within the nature of the system (aleatory, irreducible) and those sourced from our lack of knowledge(epistemic, reducible) including measurement and modeling errors. The Gamma, Lognormal, and Weibull distributions are three widely used probability distribution functions for modeling environmental loads such as winds and waves. Based on extensive literature data analysis, it is found that the Weibull distribution is a well-accepted representation of the wind speed, while the Gamma distribution is mostly used for the wave height and period. The probability of failure could significantly be underestimated if environmental load uncertainties are not considered.
- Uncertainties in structures, materials, manufacturing, and construction: to reduce the overall uncertainty of FOWTs, safety measures such as inspection, quality control, and condition monitoring might be applied during their manufacturing and operation. Literature shows up to 39% of underestimation of the probability of failure due to neglecting the uncertainties of material and geometric uncertainties. This threatens the safety of the FOWT systems.
- Geotechnical Uncertainties: soil properties exhibit high uncertainty due to the logistical issues of conducting detailed soil sampling at FOWT locations. In addition, time-varying oceanic currents and waves make the scour problem more complicated than fixed-type offshore wind turbines. This can significantly affect the stiffness, fatigue reliability, and natural frequency of FOWT support structures. Yet, soil property is one of the least investigated parameters in a probabilistic manner. Because of the computational efficiency, Gaussian probability distribution is generally applied to partially model the variabilities in soil properties. Similarly, the p-y method is widely used for the structural reliability analysis of FOWTs. However, the p-y method is incapable of precisely capturing the soil behavior. Finite element analysis could be used to accurately model the soil.
- Growing uncertainties over time: the failure mode of FOWT structures can be governed by several time-dependent phenomena including fatigue and corrosion damages, leading to the material's degradation which ultimately degrades the FOWT structure resistance. Literature shows the importance of the growing uncertainties over a lifetime. Currently, the increasing uncertainties are not taken into account in the prevailing practice. Instead, the long-term environmental loads and fatigue reliability are commonly assessed without accounting for the changing nature of uncertainties over time. The research area is recognized for its lack of existing knowledge and the need for improvement.

Future Prospects.

- To assess the reliability of FOWT structures through probabilistic
 approaches, extensive experimental data is required. Therefore,
 further numerical and experimental studies are needed for the risk
 assessment of FOWTs. Besides, since probabilistic models using a
 Bayesian approach require a large database for accurate estimation
 of the posterior probability, a combination of machine learning and
 Bayesian inference might be studied in future reliability research.
- Extreme oceanic environments and difficulty of access are considered two main disadvantages of FOWTs, resulting in a significant increase in operation and maintenance costs. Therefore, the application of condition monitoring (CM) and structural health monitoring (SHM) might be further investigated to improve safety by providing insights into the condition of FOWT structures. This may optimize the inspection intervals over FOWTs' typical service life of 20–50 years which significantly reduces the economic losses due to

lower turbine downtime. In addition, data obtained from SHM and CM might be integrated with reliability assessment to achieve target reliability indices.

Declaration of competing interest

The authors declare there are no competing finacial interests. The financial support of the work is listed under Acknowledgements.

Data availability

No data was used for the research described in the article.

Acknowledgments

This work was supported by the National Science Foundation of the U.S.A [grant number # 2118586]

Appendix

Probability distribution Function	Equation
Normal probability distribution function	$f(x) = \frac{1}{\sigma\sqrt{2\pi}} \times e^{-\frac{(x-\mu)^2}{2\sigma^2}}$
Lognormal probability distribution function	$f(x) = \frac{1}{x\sigma\sqrt{2\pi}} \times e^{-\frac{(Lnx - \mu)^2}{2\sigma^2}}$
2-parameter Weibull probability distribution function	$f(x) = \frac{k}{c} \left(\frac{x}{c}\right)^{k-1} \times e^{-\left(\frac{x}{c}\right)^{k}}$
3-parameter Weibull probability distribution function	$f(x) = \frac{k}{c} \left(\frac{x - \gamma}{c}\right)^{k-1} \times e^{-\left(\frac{x - \gamma}{c}\right)^{k}}$
Gumbel probability distribution function	$f(x) = \frac{1}{c} \times e^{-\frac{x-\gamma}{c}} - e^{\frac{x-\gamma}{c}}$
Gamma probability distribution function	$f(x) = \frac{\theta^k}{\Gamma(k)} \times x^{k-1} e^{-\theta x}$
Generalized extreme value distribution function	-1 $r-r$ $\frac{-1}{r}$
Von Mises distribution function	$f(x) = \frac{1}{c} \left[\left(1 + k \left(\frac{x - \gamma}{c} \right) \right)^{\frac{-1}{k}} \right]^{k+1} \times e^{-\left(1 + k \left(\frac{x - \gamma}{c} \right) \right)^{\frac{-1}{k}}}$ $f(x) = \frac{e^{K \cos(x - \mu)}}{2\pi I_0(K)}$

 μ : mean value, σ : standard deviation, γ : location parameter; c: scale parameter, k: shape parameter, Γ (): Gamma function, θ : rate parameter, K: concentration parameter, $I_0(K)$: modified Bessel function.

References

- Global Wind Report. Drishti IAS. 2022. https://www.drishtiias.com/daily-news-a nalysis/global-wind-report-2022. [Accessed 6 December 2022].
- [2] U.S. Energy Information Administration. Monthly energy review April 2022.
- [3] Wiser R, Lantz E, Mai T, Zayas J, DeMeo E, Eugeni E, et al. Wind vision: a new era for wind power in the United States. Elsevier; 2015.
- [4] Eriksen R, Engel D, Haugen U, Hodne T, Hovem L, Alvik S, et al. Energy Transition Outlook 2021: technology Progress report. 2021.
- [5] Wang L, Kolios A, Liu X, Venetsanos D, Rui C. Reliability of offshore wind turbine support structures: a state-of-the-art review. Renew Sustain Energy Rev 2022; 161:112250.
- [6] Jiang Z. Installation of offshore wind turbines: a technical review. Renew Sustain Energy Rev 2021;139:110576.
- [7] Sánchez S, López-Gutiérrez J-S, Negro V, Esteban MD. Foundations in offshore wind farms: Evolution, characteristics and range of use. Analysis of main dimensional parameters in monopile foundations. J Mar Sci Eng 2019;7:441.
- [8] Farr H, Ruttenberg B, Walter RK, Wang Y-H, White C. Potential environmental effects of deepwater floating offshore wind energy facilities. Ocean Coast Manag 2021;207:105611.
- [9] Barrera C, Battistella T, Guanche R, Losada IJ. Mooring system fatigue analysis of a floating offshore wind turbine. Ocean Eng 2020;195:106670.
- [10] WindEurope. Floating offshore wind energy: a policy blueprint for Europe. Position Pap 2018;10.

- [11] Raed K, Teixeira AP, Soares CG. Uncertainty assessment for the extreme hydrodynamic responses of a wind turbine semi-submersible platform using different environmental contour approaches. Ocean Eng 2020;195:106719.
- [12] Yeter B, Garbatov Y. Structural integrity assessment of fixed support structures for offshore wind turbines: a review. Ocean Eng 2022;244:110271.
- [13] Wang S, Moan T, Jiang Z. Influence of variability and uncertainty of wind and waves on fatigue damage of a floating wind turbine drivetrain. Renew Energy 2022;181:870–97.
- [14] Okpokparoro S, Sriramula S. Uncertainty modeling in reliability analysis of floating wind turbine support structures. Renew Energy 2021;165:88–108.
- [15] Jiang Z, Hu W, Dong W, Gao Z, Ren Z. Structural reliability analysis of wind turbines: a review. Energies 2017;10:2099.
- [16] Cockerill TT, Kühn M, Van Bussel GJW, Bierbooms W, Harrison R. Combined technical and economic evaluation of the Northern European offshore wind resource. J Wind Eng Ind Aerodyn 2001;89:689–711.
- [17] Zhang X, Sun L, Sun H, Guo Q, Bai X. Floating offshore wind turbine reliability analysis based on system grading and dynamic FTA. J Wind Eng Ind Aerodyn 2016;154:21–33.
- [18] Koo P, Kim H, Lim H-J, Lai L, Jang H, Jeong C. Life cycle response analysis of a floating offshore wind turbine. American Society of Mechanical Engineers; 2022.
- [19] Jonkman J, Shaler K, Wiley W, Robertson A. Sensitivity analysis of floating offshore wind turbine fatigue and ultimate loads to environmental and system property variations. Boston, Massachusetts: Northeastern University; 2022.
- [20] Toft HS, Sørensen JD. Reliability-based design of wind turbine blades. Struct Saf 2011;33:333–42.
- [21] Der Kiureghian A, Liu P-L. Structural reliability under incomplete probability information. J Eng Mech 1986;112:85–104.

- [22] Faes M, Moens D. Recent trends in the modeling and quantification of nonprobabilistic uncertainty. Arch Comput Methods Eng 2020;27:633–71.
- [23] Raftery P, Tindal A, Wallenstein M, Johns J, Warren B, Vaz F. Understanding the risks of financing wind farms. 1999. p. 496–9.
- [24] Brower MC. A Pratical Guide to developing a wind project. 2012.
- [25] Watson S, Kritharas P, Hodgson G. Wind speed variability across the UK between 1957 and 2011. Wind Energy 2015;18:21–42.
- [26] Pullinger D, Zhang M, Hill N, Crutchley T. Improving uncertainty estimates: interannual variability in Ireland, vol. 926. IOP Publishing; 2017, 012006.
- [27] Pryor S, Barthelmie RJ, Schoof J. Inter-annual variability of wind indices across Europe. Wind Energy Int J Prog Appl Wind Power Convers Technol 2006;9: 27–38.
- [28] Pryor SC, Shepherd TJ, Barthelmie RJ. Interannual variability of wind climates and wind turbine annual energy production. Wind Energy Sci 2018;3:651–65.
- [29] Hamlington B, Hamlington P, Collins S, Alexander S, Kim K. Effects of climate oscillations on wind resource variability in the United States. Geophys Res Lett 2015;42:145–52.
- [30] Früh W-G. Long-term wind resource and uncertainty estimation using wind records from Scotland as example. Renew Energy 2013;50:1014–26.
- [31] Richter P, Wolters J, Çakar R, Verhoeven-Mrosek A, Frank M. Uncertainty quantification of offshore wind farms. Wind Energy 2017;1–21.
- [32] Brower MC, Robinson NM. The openWind deep-array wake model: development and validation. AWS Truepower; 2012.
- [33] Jensen NO. A note on wind generator interaction, vol. 2411. Citeseer; 1983.
- [34] Ainslie JF. Calculating the flowfield in the wake of wind turbines. J Wind Eng Ind Aerodyn 1988;27:213–24.
- [35] Ott S. Fast linearized models for wind turbine wakes, vol. 508; 2009. p. 11-3.
- [36] Stovall T, Pawlas G, Moriarty P. Wind farm wake simulations in OpenFOAM. 2010. p. 825.
- [37] Ouarda TBMJ, Charron C, Shin J-Y, Marpu PR, Al-Mandoos AH, Al-Tamimi MH, et al. Probability distributions of wind speed in the UAE. Energy Convers Manag 2015;93:414–34. https://doi.org/10.1016/j.enconman.2015.01.036.
- [38] International Electrotechnical Commission. Wind turbine generator systems—Part 12: wind turbine power performance testing. IEC Stand Publ IEC 1998:61400. –12.
- [39] Wais P. A review of Weibull functions in wind sector. Renew Sustain Energy Rev 2017;70:1099–107. https://doi.org/10.1016/j.rser.2016.12.014.
- [40] Li Y, Huang X, Tee KF, Li Q, Wu X-P. Comparative study of onshore and offshore wind characteristics and wind energy potentials: a case study for southeast coastal region of China. Sustain Energy Technol Assess 2020;39:100711.
- [41] Saeed MK, Salam A, Rehman AU, Saeed MA. Comparison of six different methods of Weibull distribution for wind power assessment: a case study for a site in the Northern region of Pakistan. Sustain Energy Technol Assess 2019;36:100541.
- [42] Hübler C, Gebhardt CG, Rolfes R. Development of a comprehensive database of scattering environmental conditions and simulation constraints for offshore wind turbines. Wind Energy Sci 2017;2:491–505.
- [43] Fischer T, De Vries W, Schmidt B. UpWind Design Basis (WP4: offshore foundations and support structures). 2010.
- [44] Kim DH, Lee SG. Reliability analysis of offshore wind turbine support structures under extreme ocean environmental loads. Renew Energy 2015;79:161–6.
- [45] Horn J-T, Leira BJ. Fatigue reliability assessment of offshore wind turbines with stochastic availability. Reliab Eng Syst Saf 2019;191:106550.
- [46] Horn J-T, Bitner-Gregersen E, Krokstad JR, Leira BJ, Amdahl J. A new combination of conditional environmental distributions. Appl Ocean Res 2018; 73:17–26
- [47] Shu Z, Li Q, Chan P. Investigation of offshore wind energy potential in Hong Kong based on Weibull distribution function. Appl Energy 2015;156:362–73.
- [48] Pacheco A, Gorbeña E, Sequeira C, Jerez S. An evaluation of offshore wind power production by floatable systems: a case study from SW Portugal. Energy 2017; 131:239–50.
- [49] Lee ME, Kim G, Jeong S-T, Ko DH, Kang KS. Assessment of offshore wind energy at Younggwang in Korea. Renew Sustain Energy Rev 2013;21:131–41.
- [50] Zhao Y, Lian J, Lian C, Dong X, Wang H, Liu C, et al. Stochastic dynamic analysis of an offshore wind turbine structure by the path integration method. Energies 2019;12:3051.
- [51] Li H, Hu Z, Wang J, Meng X. Short-term fatigue analysis for tower base of a spartype wind turbine under stochastic wind-wave loads. Int J Nav Archit Ocean Eng 2018;10:9–20.
- [52] Ivanhoe R, Wang L, Kolios A. Generic framework for reliability assessment of offshore wind turbine jacket support structures under stochastic and time dependent variables. Ocean Eng 2020;216:107691.
- [53] Soukissian TH, Tsalis C. Effects of parameter estimation method and sample size in metocean design conditions. Ocean Eng 2018;169:19–37.
- [54] Dong S, Tao S, Li X, Soares CG. Trivariate maximum entropy distribution of significant wave height, wind speed and relative direction. Renew Energy 2015; 78:538–49.
- [55] Montes-Iturrizaga R, Heredia-Zavoni E, Silva-González F, Straub D. Nested reliability analysis of mooring lines for floating systems. Appl Ocean Res 2012;34: 107–15.
- [56] Leimeister M, Kolios A. Reliability-based design optimization of a spar-type floating offshore wind turbine support structure. Reliab Eng Syst Saf 2021;213: 107666.
- [57] Uzunoglu E, Soares CG. Yaw motion of floating wind turbine platforms induced by pitch actuator fault in storm conditions. Renew Energy 2019;134:1056–70.

- [58] Stewart GM, Robertson A, Jonkman J, Lackner MA. The creation of a comprehensive metocean data set for offshore wind turbine simulations. Wind Energy 2016;19:1151–9.
- [59] Li X, Zhang W. Long-term assessment of a floating offshore wind turbine under environmental conditions with multivariate dependence structures. Renew Energy 2020;147:764–75.
- [60] Yaniktepe B, Koroglu T, Savrun M. Investigation of wind characteristics and wind energy potential in Osmaniye, Turkey. Renew Sustain Energy Rev 2013;21: 703–11.
- [61] Carta JA, Bueno C, Ramírez P. Statistical modelling of directional wind speeds using mixtures of von Mises distributions: case study. Energy Convers Manag 2008;49:897–907.
- [62] Akpinar S, Akpinar EK. Estimation of wind energy potential using finite mixture distribution models. Energy Convers Manag 2009;50:877–84.
- [63] Pobočíková I, Sedliačková Z, Michalková M. Application of four probability distributions for wind speed modeling. Procedia Eng 2017;192:713–8.
- [64] Altunkaynak A, Erdik T, Dabanlı İ, Şen Z. Theoretical derivation of wind power probability distribution function and applications. Appl Energy 2012;92:809–14.
- [65] Rocha PAC, de Sousa RC, de Andrade CF, da Silva MEV. Comparison of seven numerical methods for determining Weibull parameters for wind energy generation in the northeast region of Brazil. Appl Energy 2012;89:395–400.
- [66] Keyhani A, Ghasemi-Varnamkhasti M, Khanali M, Abbaszadeh R. An assessment of wind energy potential as a power generation source in the capital of Iran, Tehran. Energy 2010;35:188–201.
- [67] Wais P. Two and three-parameter Weibull distribution in available wind power analysis. Renew Energy 2017;103:15–29.
- [68] Sørensen JD, Toft HS. Probabilistic design of wind turbines. Energies 2010;3: 241–57
- [69] Stewart D, Eeesnwanger O. Frequency distribution of wind speed near the surface. 1978.
- [70] Van der Auwera L, De Meyer F, Malet LM. The use of the Weibull three-parameter model for estimating mean wind power densities. J Appl Meteorol 1980;19: 819–25
- [71] Horn J-TH, Jensen JJ. Reducing uncertainty of Monte Carlo estimated fatigue damage in offshore wind turbines using FORM. In: Proc. 13th Int. Symp. Pract. Des. Ships Float. Struct. PRADS2016. Technical University of Denmark (DTU); 2016
- [72] Karmakar D, Bagbanci H, Guedes Soares C. Long-term extreme load prediction of spar and semisubmersible floating wind turbines using the environmental contour method. J Offshore Mech Arct Eng 2016;138.
- [73] Karimirad M, Moan T. Extreme dynamic structural response analysis of catenary moored spar wind turbine in harsh environmental conditions. J Offshore Mech Arct Eng 2011;133.
- [74] Haselsteiner AF, Coe RG, Manuel L, Chai W, Leira B, Clarindo G, et al. A benchmarking exercise for environmental contours. Ocean Eng 2021;236: 109504.
- [75] International Electrotechnical Commission. Wind turbines-part 1: design requirements. thirty zero ed. 2005. IEC 61400-1-.
- [76] Ruzzo C, Arena F. A numerical study on the dynamic response of a floating spar platform in extreme waves. J Mar Sci Technol 2019;24:1135–52.
- [77] Morison J, Johnson J, Schaaf S. The force exerted by surface waves on piles. J Pet Technol 1950:2:149–54.
- [78] Tran TT, Kim D-H. Fully coupled aero-hydrodynamic analysis of a semisubmersible FOWT using a dynamic fluid body interaction approach. Renew Energy 2016;92:244–61.
- [79] Najafian G, Burrows R, Tickell R. A review of the probabilistic description of Morison wave loading and response of fixed offshore structures. J Fluids Struct 1995;9:585-616
- [80] Raed K, Uzunoglu E, Soares CG. Uncertainty associated with the estimation of drag and inertia coefficients of fixed vertical cylinders. Prog Renew Energ Offshore Taylor Francis Group Lond UK 2016:767–74.
- [81] Raed K, Soares CG. Variability effect of the drag and inertia coefficients on the Morison wave force acting on a fixed vertical cylinder in irregular waves. Ocean Eng 2018;159:66–75.
- [82] Soares CG, Moan T. On the uncertainties related to the extreme hydrodynamic loading of a cylindrical pile. In: Reliab. Theory its Appl. Struct. Soil Mech. Springer; 1983. p. 351–64.
- [83] Moan T, Gao Z, Ayala-Uraga E. Uncertainty of wave-induced response of marine structures due to long-term variation of extratropical wave conditions. Mar Struct 2005;18:359–82.
- [84] Zhang J, Kang J, Sun L, Bai X. Risk assessment of floating offshore wind turbines based on fuzzy fault tree analysis. Ocean Eng 2021;239:109859.
- [85] Ziegler L, Voormeeren S, Schafhirt S, Muskulus M. Sensitivity of wave fatigue loads on offshore wind turbines under varying site conditions. Energy Proc 2015; 80:193–200.
- [86] Lucas C, Soares CG. Bivariate distributions of significant wave height and mean wave period of combined sea states. Ocean Eng 2015;106:341–53.
- [87] Dong S, Wang N, Liu W, Soares CG. Bivariate maximum entropy distribution of significant wave height and peak period. Ocean Eng 2013;59:86–99.
- [88] Huseby AB, Vanem E, Natvig B. A new approach to environmental contours for ocean engineering applications based on direct Monte Carlo simulations. Ocean Eng 2013;60:124–35.
- [89] Nava V, Arena F, Romolo A. Non-linear random wave groups with a superimposed current, vol. 47489; 2006. p. 229–37.

- [90] Qu X, Li Y, Tang Y, Hu Z, Zhang P, Yin T. Dynamic response of spar-type floating offshore wind turbine in freak wave considering the wave-current interaction effect. Appl Ocean Res 2020;100:102178.
- [91] Chung WC, Pestana GR, Kim M. Structural health monitoring for TLP-FOWT (floating offshore wind turbine) tendon using sensors. Appl Ocean Res 2021;113: 102740.
- [92] Clark CE, DuPont B. Reliability-based design optimization in offshore renewable energy systems. Renew Sustain Energy Rev 2018;97:390–400.
- [93] Truong HVA, Dang TD, Vo CP, Ahn KK. Active control strategies for system enhancement and load mitigation of floating offshore wind turbines: a review. Renew Sustain Energy Rev 2022;170:112958.
- [94] Zhang J, Zhang M, Jiang X, Wu L, Qin J, Li Y. Pair-Copula-based trivariate joint probability model of wind speed, wind direction and angle of attack. J Wind Eng Ind Aerodyn 2022;225:105010.
- [95] Ramadhani A, Khan F, Colbourne B, Ahmed S, Taleb-Berrouane M. A multivariate model to estimate environmental load on an offshore structure. Ocean Eng 2023; 274:114067
- [96] Haver S. On the joint distribution of heights and periods of sea waves. Ocean Eng 1987:14:359–76.
- [97] Mathisen J, Bitner-Gregersen E. Joint distributions for significant wave height and wave zero-up-crossing period. Appl Ocean Res 1990;12:93–103.
- [98] Ferreira J, Soares CG. Modelling bivariate distributions of significant wave height and mean wave period. Appl Ocean Res 2002;24:31–45.
- [99] Athanassoulis G, Skarsoulis E, Belibassakis K. Bivariate distributions with given marginals with an application to wave climate description. Appl Ocean Res 1994; 16:1–17
- [100] Haver S. Wave climate off northern Norway. Appl Ocean Res 1985;7:85-92.
- [101] Velarde J, Vanem E, Kramhøft C, Sørensen JD. Probabilistic analysis of offshore wind turbines under extreme resonant response: application of environmental contour method. Appl Ocean Res 2019;93:101947.
- [102] Good IJ. Maximum entropy for hypothesis formulation, especially for multidimensional contingency tables. Ann Math Stat 1963;34:911–34.
- [103] Fratantoni DM. North Atlantic surface circulation during the 1990's observed with satellite-tracked drifters. J Geophys Res Oceans 2001;106:22067–93.
- [104] Otter A, Flannery B, Murphy J, Desmond C. Current simulation with Software in the Loop for floating offshore wind turbines, vol. 2265. IOP Publishing; 2022, 042028.
- [105] Lsp Silva, Cazzolato B, Ny Sergiienko, Ding B. Nonlinear dynamics of a floating offshore wind turbine platform via statistical quadratization—mooring, wave and current interaction. Ocean Eng 2021;236:109471.
- [106] Van Der Tempel J, Diepeveen N, De Vries W, Salzmann DC. Offshore environmental loads and wind turbine design: impact of wind, wave, currents and ice. Wind Energy Syst., Elsevier; 2011. p. 463–78.
- [107] Lee M, Lu C, Huang H. Reliability and cost analyses of electricity collection systems of a marine current farm—a Taiwanese case study. Renew Sustain Energy Rev. 2009;13:2012–21.
- [108] Zheng Z, Chen J, Liang H, Zhao Y, Shao Y. Hydrodynamic responses of a 6 MW spar-type floating offshore wind turbine in regular waves and uniform current. Fluids 2020;5:187.
- [109] Ishihara T, Liu Y. Dynamic response analysis of a semi-submersible floating wind turbine in combined wave and current conditions using advanced hydrodynamic models. Energies 2020;13:5820.
- [110] Iec 61400-3 Ed.1. Wind turbines—Part 3: design requirements for offshore wind turbines. International Electrotechnical Commission (IEC); 2009.
- [111] Pierson Jr WJ, Moskowitz L. A proposed spectral form for fully developed wind seas based on the similarity theory of SA Kitaigorodskii. J Geophys Res 1964;69: 5181–90.
- [112] Hasselmann DE, Dunckel M, Ewing J. Directional wave spectra observed during JONSWAP 1973. J Phys Oceanogr 1980;10:1264–80.
- [113] Haid L, Stewart G, Jonkman J, Robertson A, Lackner M, Matha D. Simulation-length requirements in the loads analysis of offshore floating wind turbines, vol. 55423. American Society of Mechanical Engineers; 2013. V008T09A091.
- [114] Chen L, Basu B. Fatigue load estimation of a spar-type floating offshore wind turbine considering wave-current interactions. Int J Fatigue 2018;116:421–8.
- [115] Johannessen K, Meling TS, Hayer S. Joint distribution for wind and waves in the northern north sea. OnePetro; 2001.
- [116] Li L, Gao Z, Moan T. Joint environmental data at five european offshore sites for design of combined wind and wave energy devices, vol. 55423. American Society of Mechanical Engineers; 2013. V008T09A006.
- [117] Stewart GM. Design load analysis of two floating offshore wind turbine concepts. 2016.
- [118] Chen C, Ma Y, Fan T. Review of model experimental methods focusing on aerodynamic simulation of floating offshore wind turbines. Renew Sustain Energy Rev 2022;157:112036.
- [119] Toft HS, Branner K, Berring P, Sørensen JD. Defect distribution and reliability assessment of wind turbine blades. Eng Struct 2011;33:171–80.
- [120] GE Press Release. GE researchers Unveil 12 MW floating wind turbine concept | GE research. 2021. https://www.ge.com/research/newsroom/ge-researchers-unveil-12-mw-floating-wind-turbine-concept. [Accessed 14 December 2022].
- [121] Chou J-S, Chiu C-K, Huang I-K, Chi K-N. Failure analysis of wind turbine blade under critical wind loads. Eng Fail Anal 2013;27:99–118.
- [122] Gonzaga P, Toft H, Worden K, Dervilis N, Bernhammer L, Stevanovic N, et al. Impact of blade structural and aerodynamic uncertainties on wind turbine loads. Wind Energy 2022;25:1060–76. https://doi.org/10.1002/we.2715.

- [123] Suzuki T, Mahfuz H, Takanashi M. A new stiffness degradation model for fatigue life prediction of GFRPs under random loading. Int J Fatigue 2019;119:220–8. https://doi.org/10.1016/j.ijfatigue.2018.09.021.
- [124] Talreja R. A mechanisms-based reliability model for fatigue of composite laminates: composite fatigue reliability. ZAMM - J Appl Math Mech Z Für Angew Math Mech 2015;95:1058–66. https://doi.org/10.1002/zamm.201500047.
- [125] Lekou D, Philippidis T. PRE-and POST-THIN: a tool for the probabilistic design and analysis of composite rotor blade strength. Wind Energy Int J Prog Appl Wind Power Convers Technol 2009;12:676–91.
- [126] Hu Z, Li H, Du X, Chandrashekhara K. Simulation-based time-dependent reliability analysis for composite hydrokinetic turbine blades. Struct Multidiscip Optim 2013;47:765–81.
- [127] Mustafa G, Suleman A, Crawford C. Probabilistic micromechanical analysis of composite material stiffness properties for a wind turbine blade. Compos Struct 2015;131:905–16.
- [128] Young AC, Goupee AJ, Dagher HJ, Viselli AM. Methodology for optimizing composite towers for use on floating wind turbines. J Renew Sustain Energy 2017; 9:033305
- [129] Liu L, Bian H, Du Z, Xiao C, Guo Y, Jin W. Reliability analysis of blade of the offshore wind turbine supported by the floating foundation. Compos Struct 2019; 211:287–300
- [130] Li H, Soares CG. Assessment of failure rates and reliability of floating offshore wind turbines. Reliab Eng Syst Saf 2022;228:108777.
- [131] Shittu AA, Mehmanparast A, Amirafshari P, Hart P, Kolios A. Sensitivity analysis of design parameters for reliability assessment of offshore wind turbine jacket support structures. Int J Nav Archit Ocean Eng 2022;14:100441.
- [132] Pokhrel J, Seo J. Statistical model for fragility estimates of offshore wind turbines subjected to aero-hydro dynamic loads. Renew Energy 2021;163:1495–507.
- [133] Hsu W, Thiagarajan KP, MacNicoll M, Akers R. Prediction of extreme tensions in mooring lines of a floating offshore wind turbine in a 100-year storm. In: Int. Conf. Offshore Mech. Arct. Eng., vol. 56574. American Society of Mechanical Engineers; 2015. V009T09A050.
- [134] Hsu W, Thiagarajan KP, Manuel L. Extreme mooring tensions due to snap loads on a floating offshore wind turbine system. Mar Struct 2017;55:182–99.
- [135] Rendón-Conde C, Heredia-Zavoni E. Reliability assessment of mooring lines for floating structures considering statistical parameter uncertainties. Appl Ocean Res 2015;52:295–308.
- [136] Horte T, Lie H, Mathisen J. Calibration of an ultimate limit state for mooring lines. 1998.
- [137] Benassai G, Campanile A, Piscopo V, Scamardella A. Ultimate and accidental limit state design for mooring systems of floating offshore wind turbines. Ocean Eng 2014:92:64–74.
- [138] Carswell W, Arwade SR, DeGroot DJ, Lackner MA. Soil-structure reliability of offshore wind turbine monopile foundations. Wind Energy 2015;18:483–98.
- [139] Mardfekri M, Gardoni P. Probabilistic demand models and fragility estimates for offshore wind turbine support structures. Eng Struct 2013;52:478–87.
- [140] Rezaei R, Duffour P, Fromme P. Scour influence on the fatigue life of operational monopile-supported offshore wind turbines. Wind Energy 2018;21:683–96.
- [141] Abhinav K, Saha N. Effect of scouring in sand on monopile-supported offshore wind turbines. Mar Georesources Geotechnol 2017;35:817–28.
- [142] Ma H, Yang J, Chen L. Effect of scour on the structural response of an offshore wind turbine supported on tripod foundation. Appl Ocean Res 2018;73:179–89.
- [143] Breusers HNC, Nicollet G, Shen HW. Local scour around cylindrical Piers. J Hydraul Res 1977;15:211–52. https://doi.org/10.1080/00221687709499645.
- [144] Sumer BM. The mechanics of scour in the marine environment. World Scientific;
- [145] Patra SK, Haldar S. Seismic response of monopile supported offshore wind turbine in liquefiable soil, vol. 31. Elsevier; 2021. p. 248–65.
- [146] Jonkman J. DNV GL joint industry project on coupled analysis of floating wind turbines. Golden, CO (United States): National Renewable Energy Lab.(NREL); 2019
- [147] Zhang J, Yuan G-K, Zhu S, Gu Q, Ke S, Lin J. Seismic analysis of 10 MW offshore wind turbine with large-diameter monopile in consideration of seabed liquefaction. Energies 2022;15:2539.
- [148] Zaaijer M. Foundation modelling to assess dynamic behaviour of offshore wind turbines. Appl Ocean Res 2006;28:45–57.
- [149] Agarwal P, Manuel L. Simulation of offshore wind turbine response for long-term extreme load prediction. Eng Struct 2009;31:2236–46.
- [150] Young I, Zieger S, Babanin AV. Global trends in wind speed and wave height. Science 2011;332:451–5.
- [151] Choe D-E, Gardoni P, Rosowsky D. Fragility increment functions for deteriorating reinforced concrete bridge columns. J Eng Mech 2010;136:969–78.
- [152] Müller K, Cheng PW. Application of a Monte Carlo procedure for probabilistic fatigue design of floating offshore wind turbines. Wind Energy Sci 2018;3: 149–62.
- [153] Hübler C, Rolfes R. Analysis of the influence of climate change on the fatigue lifetime of offshore wind turbines using imprecise probabilities. Wind Energy 2021;24:275–89.
- [154] Grabemann I, Weisse R. Climate change impact on extreme wave conditions in the North Sea: an ensemble study. Ocean Dyn 2008;58:199–212.
- [155] Zeng Z, Ziegler AD, Searchinger T, Yang L, Chen A, Ju K, et al. A reversal in global terrestrial stilling and its implications for wind energy production. Nat Clim Change 2019;9:979–85.
- [156] Dong XH, Yuan TJ, Ma RH. Corrosion mechanism on offshore wind turbine blade in salt fog environment, vol. 432. Trans Tech Publ; 2013. p. 258–62.

- [157] Valamanesh V, Myers AT, Arwade SR. Multivariate analysis of extreme metocean conditions for offshore wind turbines. Struct Saf 2015;55:60–9.
- [158] Vorpahl F, Schwarze H, Fischer T, Seidel M, Jonkman J. Offshore wind turbine environment, loads, simulation, and design, vol. 2. Wiley Interdiscip Rev Energy Environ; 2013. p. 548–70.
- [159] Wind Power Monthly. Chinese typhoon knocks out 17 wind turbines. 2013. https://www.windpowermonthly.com/article/1213452/chinese-typhoon-knocks-17-wind-turbines?utm_source=website&utm_medium=social. [Accessed 13 December 2022].
- [160] Yeter B, Garbatov Y, Soares CG. Fatigue reliability of an offshore wind turbine supporting structure accounting for inspection and repair. Anal Des Mar Struct Soares G Shenoi E; 2015. p. 737–47.
- [161] Dong P, Hong JK, Osage DA, Prager M. Master SN curve method for fatigue evaluation of welded components. Weld Res Counc Bull 2002; 474: 1-50.
- [162] Anderson TL. Fracture mechanics: fundamentals and applications. CRC press;
- [163] Schløer S, Bredmose H, Bingham HB. The influence of fully nonlinear wave forces on aero-hydro-elastic calculations of monopile wind turbines. Mar Struct 2016; 50:162-88.
- [164] Kvittem MI, Moan T. Frequency versus time domain fatigue analysis of a semisubmersible wind turbine tower. J Offshore Mech Arct Eng 2015;137.
- [165] Ralby I, Bochman A. Cybersecurity CONCERNS for the energy sector IN the MARITIME DOMAIN. Atl Counc Issue Pap 2021:1.
- [166] Liu Y, Li S, Chan PW, Chen D. On the failure probability of offshore wind turbines in the China coastal waters due to typhoons: a case study using the OC4– DeepCwind semisubmersible. IEEE Trans Sustain Energy 2018;10:522–32.
- [167] Sheng C, Hong H. Reliability and fragility assessment of offshore floating wind turbine subjected to tropical cyclone hazard. Struct Saf 2021;93:102138.
- [168] Tarp-Johansen N, Sørensen JD, Madsen PH. Experience with acceptance criteria for offshore wind turbines in extreme loading. 2002.
- [169] Sørensen JD. Reliability assessment of wind turbines. 2015.
- [170] Toft HS, Sørensen JD. Stochastic models for strength of wind turbine blades using tests. The European Wind Energy Association; 2008.
- [171] Ramezani M, Kim YH, Sun Z. Probabilistic model for flexural strength of cementitious materials containing CNTs. 2020.
- [172] Ramezani M, Kim YH, Sun Z. Probabilistic model for flexural strength of carbon nanotube reinforced cement-based materials. Compos Struct 2020;253:112748.
- [173] Ramezani M, Kim YH, Sun Z. Elastic modulus formulation of cementitious materials incorporating carbon nanotubes: probabilistic approach. Constr Build Mater 2021;274:122092.
- [174] DNVGL-ST-0126. DNVGL-ST-0126: support structures for wind turbines. Oslo Nor DNV GL: 2016.
- [175] Gardoni P, Der Kiureghian A, Mosalam KM. Probabilistic capacity models and fragility estimates for reinforced concrete columns based on experimental observations. J Eng Mech 2002;128:1024–38.
- [176] Choe D-E, Gardoni P, Rosowsky D, Haukaas T. Probabilistic capacity models and seismic fragility estimates for RC columns subject to corrosion. Reliab Eng Syst Saf 2008:93:383–93
- [177] Choe D-E, Gardoni P, Rosowsky D, Haukaas T. Seismic fragility estimates for reinforced concrete bridges subject to corrosion. Struct Saf 2009;31:275–83.
- [178] Melchers RE, Beck AT. Structural reliability analysis and prediction. John wiley & sons: 2018.
- [179] Tokdar ST, Kass RE. Importance sampling: a review, vol. 2. Wiley Interdiscip Rev Comput Stat; 2010. p. 54–60.
- [180] Olsson A, Sandberg G, Dahlblom O. On Latin hypercube sampling for structural reliability analysis. Struct Saf 2003;25:47–68.
- [181] Au S-K, Beck JL. Estimation of small failure probabilities in high dimensions by subset simulation. Probabilistic Eng Mech 2001;16:263–77.
- [182] Melchers RE. Structural system reliability assessment using directional simulation. Struct Saf 1994:16:23–37.
- [183] Gilks WR, Richardson S, Spiegelhalter D. Markov chain Monte Carlo in practice. CRC press; 1995.
- [184] Huang C, El Hami A, Radi B. Overview of structural reliability analysis methods—Part I: local reliability methods. Incert Fiabilité Systèmes Multiphysiques 2017;17:1–10.
- [185] Der Kiureghian A, Lin H-Z, Hwang S-J. Second-order reliability approximations. J Eng Mech 1987;113:1208–25.

- [186] Echard B, Gayton N, Lemaire M, Ak-Mcs. An active learning reliability method combining Kriging and Monte Carlo simulation. Struct Saf 2011;33:145–54.
- [187] Bichon BJ, Eldred MS, Swiler LP, Mahadevan S, McFarland JM. Efficient global reliability analysis for nonlinear implicit performance functions. AIAA J 2008;46: 2459-68
- [188] Mardfekri M, Gardoni P, Bisadi V. Service reliability of offshore wind turbines. Int J Sustain Energy 2015;34:468–84.
- [189] Agarwal P, Manuel L. Incorporating irregular nonlinear waves in coupled simulation and reliability studies of offshore wind turbines. Appl Ocean Res 2011; 33:215–27.
- [190] Gaertner EM, Lackner MA. Aero-elastic design optimization of floating offshore wind turbine blades. Wind Energy Symp.; 2018. p. 2015. 2018.
- [191] Choe D-E, Kim H-C, Kim M-H. Sequence-based modeling of deep learning with LSTM and GRU networks for structural damage detection of floating offshore wind turbine blades. Renew Energy 2021;174:218–35.
- [192] Garbatov Y, Soares CG. Bayesian updating in the reliability assessment of maintained floating structures. J Offshore Mech Arct Eng 2002;124:139–45.
- [193] Zhao Y, Dong S. Comparison of environmental contour and response-based approaches for system reliability analysis of floating structures. Struct Saf 2022; 94:102150
- [194] Basu RI, Bhattacharya B. Challenges in the application of system reliability Principles to floating structures. 24th Meeting of the United States Japan Natural Resources Marine Facilities Panel 2001;2001:1–12.
- [195] Dnv G. Offshore standard DNVGL-OS-E301 position mooring. DNV GL 2018:
- [196] Hou H-M, Liu Y, Dong G-H, Xu T-J. Reliability assessment of mooring system for fish cage considering one damaged mooring line. Ocean Eng 2022;257:111626. https://doi.org/10.1016/j.oceaneng.2022.111626.
- [197] Liu H, Zhao C, Ma G, He L, Sun L, Li H. Reliability assessment of a floating offshore wind turbine mooring system based on the TLBO algorithm. Appl Ocean Res 2022;124:103211. https://doi.org/10.1016/j.apor.2022.103211.
- [198] Zhao Y, Dong S, Jiang F. Reliability analysis of mooring lines for floating structures using ANN-BN inference. Proc Inst Mech Eng Part M J Eng Marit Environ 2021;235:236–54. https://doi.org/10.1177/1475090220925200.
- [199] Andrawus JA, Mackay L. Offshore wind turbine blade coating deterioration maintenance model. Wind Eng 2011;35:551–60.
- [200] Dong W, Moan T, Gao Z. Fatigue reliability analysis of the jacket support structure for offshore wind turbine considering the effect of corrosion and inspection. Reliab Eng Syst Saf 2012;106:11–27.
- [201] Shittu AA, Mehmanparast A, Shafiee M, Kolios A, Hart P, Pilario K. Structural reliability assessment of offshore wind turbine support structures subjected to pitting corrosion-fatigue: a damage tolerance modelling approach. Wind Energy 2020:23:2004–26.
- [202] Tarp-Johansen NJ, Clausen N-E. Design of Wind Turbines in Typhoon area: a first study of structural safety of wind turbines in typhoon prone areas. 2006.
- [203] Rose S, Jaramillo P, Small MJ, Grossmann I, Apt J. Quantifying the hurricane risk to offshore wind turbines. Proc Natl Acad Sci 2012;109:3247–52.
- [204] Mardfekri M, Gardoni P. Multi-hazard reliability assessment of offshore wind turbines. Wind Energy 2015;18:1433–50.
- [205] Katsanos EI, Sanz AA, Georgakis CT, Thöns S. Multi-hazard response analysis of a 5MW offshore wind turbine. Procedia Eng 2017;199:3206–11.
- [206] Velarde J, Kramhøft C, Sørensen JD, Zorzi G. Fatigue reliability of large monopiles for offshore wind turbines. Int J Fatigue 2020;134:105487.
 [207] Vahdatirad MJ, Griffiths D, Andersen LV, Sørensen JD, Fenton G. Reliability
- [207] Vahdatirad MJ, Griffiths D, Andersen LV, Sørensen JD, Fenton G. Reliability analysis of a gravity-based foundation for wind turbines: a code-based design assessment. Geotechnique 2014;64:635–45.
- [208] Morató A, Sriramula S. Calibration of safety factors for offshore wind turbine support structures using fully coupled simulations. Mar Struct 2021;75:102880.
- [209] Li X, Zhang W. Long-term fatigue damage assessment for a floating offshore wind turbine under realistic environmental conditions. Renew Energy 2020;159: 570-84
- [210] Gao J, Yuan Y. Probabilistic modeling of stiffness degradation for fiber reinforced polymer under fatigue loading. Eng Fail Anal 2020;116:104733. https://doi.org/ 10.1016/j.engfailanal.2020.104733.
- [211] Yang J-N, Trapp W. Reliability analysis of aircraft structures under random loading and periodic inspection. AIAA J 1974;12:1623–30.